Complex life cycles drive community assembly through immigration and adaptive diversification

Marco Saltini[1,2], Paula Vasconcelos[1], and Claus Rueffler[1]

1. Department of Ecology and Genetics, Animal Ecology, Uppsala University, Norbyvägen 18D, 752 36 Uppsala, Sweden
2. Swedish Collegium for Advanced Study (SCAS), Thunbergsvägen 2, 752 38 Uppsala, Sweden

email addresses: marco.saltini@ebc.uu.se, paula.vasconcelos@ebc.uu.se, claus.rueffler@ebc.uu.se

Short running title: Complex life cycles and community assembly

Keywords: adaptive dynamics, coexistence, evolutionary branching, immigration, ontogentic niche shift.

Type of article: Letter

Number of words in the abstract: 147

Number of words in the main text: 4683

Number of figures and tables: 5 figures

Number of references: 70

Corresponding author: Marco Saltini, marco.saltini@ebc.uu.se

Authorship contribution

Marco Saltini: Conceptualization, Formal Analysis, Writing - original draft, review and editing. *Paula Vasconcelos:* Conceptualization, Writing - review and editing. *Claus Rueffler:* Conceptualization, Writing - original draft, review and editing, Supervision.

Data availability statement

The simulations code used in this study is available from the corresponding author upon reasonable request. Should the manuscript be accepted, the simulations code will be archived in an appropriate public repository. No new data were used.

Conflict of interest

The authors declare that they have no known competing financial interests or personal relationships that could have appeared to influence the work reported in this paper.

Abstract

Most animals undergo ontogentic niche shifts during their life. Yet, standard ecological theory builds on models that ignore this complexity. Here, we study how complex life cycles, where juvenile and adult individuals each feed on different sets of resources, affect community richness. Two different modes of community assembly are considered: gradual adaptive evolution and immigration of new species with randomly selected phenotypes. We find that under gradual evolution complex life cycles can lead to both higher and lower species richness when compared to a model of species with simple life cycles that lack an ontogenetic niche shift. Thus, complex life cycles do not *per se* increase the scope for gradual adaptive diversification. However, complex life cycles can lead to significantly higher species richness when communities are assembled trough immigration, as immigrants can occupy isolated peaks of the dynamic fitness landscape that are not accessible via gradual evolution.

Introduction

In his classic review, Wilbur (1980) defines a *complex life cycle* as "a life history that includes an abrupt ontogenetic change in an individual's morphology, physiology, and behavior, usually associated with a change in habitat". Wilbur adds that "the changes that accompany metamorphosis are often sufficiently radical for an ecologist to declare that the species sequentially occupies two niches", a phenomenon known as *ontogenetic niche shift*. Complex life cycles characterize anurans, insects, and many marine invertebrates, and Werner (1988) estimates that more than 80% of all animals have complex life cycles with an ontogenetic niche shift. Additionally, Werner & Gilliam (1984) suggest that a large proportion of direct developing species have effectively complex life cycles since they exhibit marked niche shifts during their ontogeny. Consequently, Werner (1988) concludes that complex life cycles should be considered the norm among animals. The phenomenon of ontogenetic niche shifts is not restricted to animals but also recognized in plants (e.g., Eriksson, 2002; Lasky *et al.*, 2015; Parrish & Bazzaz, 1985).

The consequences of complex life cycles and ontogentic niche shifts for community richness are potentially significant (for reviews, see Miller & Rudolf, 2011; Moran, 1994; Nakazawa, 2015; Wilbur, 1980). From an ecological perspective, recent empirical research focused on the role of ontogentic niche shifts for species coexistence in plant communities (Lasky *et al.*, 2015), freshwater invertebrates (Rudolf & Eveland, 2021), and fish (Anaya-Rojas *et al.*, 2021). From an evolutionary perspective, several authors provide evidence that complex life cycles could drive high speciation rates in amphibians (Bossuyt & Milinkovitch, 2000) and insects (Mayhew, 2007; Rainford *et al.*, 2014; Yang, 2001).

Existing theory including complex life cycles covers topics such as the evolutionary origin of complex life cycles (Ebenman, 1992; Istock, 1967; Landi *et al.*, 2018; ten Brink *et al.*, 2019), the consequences of complex life cycles for food web stability (Mougi, 2017; de Roos, 2021; Rudolf & Lafferty, 2011), the coexistence of prey species (Wollrab *et al.*, 2013), the ecological coupling across habitats (Nakazawa, 2011; Schreiber & Rudolf, 2008), and the complex population dynamics arising from the usage of different resources at different stages (Nakazawa, 2015; de Roos & Persson, 2013; Schreiber & Rudolf, 2008). However, only a small number of studies addresses how complex life cycles affect ecological speciation (Claessen & Dieckmann, 2002), coexistence of competing species, and character displacement, all integral topics in ecology and evolutionary ecology. In particular, in the wake of Robert MacArthur seminal work (MacArthur, 1972; MacArthur & Levins, 1967), theorizing on these latter questions has been dominated by models describing the population dynamics of unstructured populations (e.g., Abrams, 1986; Dieckmann & Doebeli, 1999; McPeek, 2022; Taper & Case, 1992).

The few studies that do investigate the consequences of complex life cycles for coexistence of competing species focus on just two species, where density-dependent population regulation at the juvenile and adult stage arises from competition for a single stage-specific resource (Hassell & Comins, 1976; Loreau & Ebenhöh, 1994; Moll & Brown, 2008; Schellekens *et al.*, 2010). The common finding from these models is that two species can coexist if one is more regulated at the juvenile stage and the other more regulated at the adult stage. A very different approach has most recently been taken by ten Brink & Seehausen (2022), who study adaptive radiations in species with complex life cycles under the assumption that small individuals feed on a shared resource while large individuals have access to multiple resources on which they can specialize. They find that ontogentic niche shifts can hinder diversification.

Here, we study evolutionary diversification, coexistence, and character displacement for consumer

species with complex life cycles. Ontogenetic niche shifts are incorporated by assuming that juvenile and adult individuals forage on stage-specific distributions of self-renewing resources with efficiencies that depend on a juvenile and adult foraging trait. Specifically, we ask how ontogentic niche shifts affect the maximum number of consumer species that can coexist in a single community, where species are characterized by the values of their juvenile and adult foraging trait. We address this question for two modes of community assembly. First, under gradual evolution, diversity builds up within the community through repeated mutations of small phenotypic effect through a sequence of evolutionary branching events (Doebeli, 2011; Geritz *et al.*, 1998). Here, we study the endpoint of an adaptive radiation that is driven by negative frequency-dependent selection arising from competition for shared resources. Second, under immigration, we repeatedly add immigrants with random phenotypes until no further immigrant can successfully establish itself in the community. We then compare species richness and phenotypic composition of the final communities arising under the two modes of community assembly, both with each other and with the corresponding results from a model in which species have simple life cycles without ontogenetic niche shifts.

We find that the role of complex life cycles in species richness depends on the mode of community assembly. Adding life cycle complexity increases species richness in gradual adaptive radiations only if individuals in at least one of the life stages have a narrower feeding niche width than individuals with a simple life cycle. However, introducing life cycle complexity adds many potential fitness peaks to a variable fitness landscape that are not reachable through gradual evolution, resulting in unsaturated communities. If communities are assembled through sequential immigration these fitness peaks become occupied, and communities of species with complex life cycles are significantly richer than communities of species with simple life cycles.

The model

To investigate how complex life cycles affect community assembly, we introduce a continuous time ecological model for n consumer species with a life cycle consisting of two different life stages, referred to as juveniles and adults, that feed on stage-specific continuous distributions of self-renewing resources. The depletion of these resources due to consumption mediates the interaction between consumer species and governs community assembly.

Population dynamics

Our ecological model is an extension of the consumer-resource model by Schreiber & Rudolf (2008), and a schematic representation is shown in Figure 1. Juvenile and adult individuals forage on stage-specific continuous resource distributions, with resources characterized by a real-valued trait z. The density of resource items of type z that are available to juvenile and adult consumers is denoted by $R_J(z)$ and $R_A(z)$, respectively. In the absence of consumers, resources grow logistically with trait-independent intrinsic growth rates r_J and r_A to the trait-dependent carrying capacities $K_J(z)$ and $K_A(z)$, assumed to be Gaussian functions centred around $z = 0$, i.e.,

$$K_J(z) = k_J \exp\left(-\frac{z^2}{2\omega_J^2}\right), \tag{1a}$$

$$K_A(z) = k_A \exp\left(-\frac{z^2}{2\omega_A^2}\right), \tag{1b}$$

where k_J and k_A are stage-specific scaling factors, and ω_J^2 and ω_A^2 describe the width of the resource distributions in the absence of consumers.

Juvenile and adult consumers are characterized by a real valued trait x^J and x^A, respectively. Hereafter, we refer to these trait values as the niche position of juveniles and adults. The trait values determine the resource type that juveniles and adults, respectively, utilize most efficiently according to the feeding efficiency functions $a_J(z, x^J)$ and $a_A(z, x^A)$, assumed to be monotonically increasing with decreasing distance between the consumer and resource trait values. For the sake of mathematical tractability, we choose the Gaussian functions

$$a_J(z, x^J) = \frac{1}{\sqrt{2\pi\sigma_J^2}} \exp\left[-\frac{\left(x^J - z\right)^2}{2\sigma_J^2}\right], \tag{2a}$$

$$a_A(z, x^A) = \frac{1}{\sqrt{2\pi\sigma_A^2}} \exp\left[-\frac{\left(x^A - z\right)^2}{2\sigma_A^2}\right], \tag{2b}$$

where σ_J^2 and σ_A^2 are the widths of the juvenile and adult feeding efficiency functions, respectively, hereafter referred to as juvenile and adult niche width for short.

The two trait values characterizing a consumer are collected in a trait vector $\boldsymbol{x} = (x^J, x^A)$. To distinguish between the n different consumer species of a community we add the subscript $i \in \{1, \ldots, n\}$ to the trait values, $\boldsymbol{x}_i = (x_i^J, x_i^A)$. The density of juveniles and adults with trait value x_i^J and x_i^A are denoted by J_i and A_i, respectively. Juveniles and adults consume resources according to a linear functional response. Maturation of juveniles into adults and birth of new juveniles occur at rates proportional to the rate of resource consumption. The proportionality constant is given by the stage-specific conversion efficiencies c_J and c_A, which are assumed to be independent on the resource trait value. Finally, juveniles and adults die at stage-specific death rates d_J and d_A. With this, the dynamics of resource density for resources of type z in the presence of n consumer species is given by

$$\frac{\mathrm{d}R_J(z)}{\mathrm{d}t} = R_J(z)r_J\left(1 - \frac{R_J(z)}{K_J(z)}\right) - R_J(z)\sum_{i=1}^{n} a_J(z, x_i^J)J_i \tag{3a}$$

$$\frac{\mathrm{d}R_A(z)}{\mathrm{d}t} = R_A(z)r_A\left(1 - \frac{R_A(z)}{K_A(z)}\right) - R_A(z)\sum_{i=1}^{n} a_A(z, x_i^A)A_i, \tag{3b}$$

whereas the dynamics of the density of juveniles and adult consumers of species i is described by

$$\frac{\mathrm{d}J_i}{\mathrm{d}t} = A_i c_A \int_{-\infty}^{+\infty} a_A(z, x_i^A)R_A(z)\mathrm{d}z - J_i c_J \int_{-\infty}^{+\infty} a_J(z, x_i^J)R_J(z)\mathrm{d}z - J_i d_J, \tag{4a}$$

$$\frac{\mathrm{d}A_i}{\mathrm{d}t} = J_i c_J \int_{-\infty}^{+\infty} a_J(z, x_i^J)R_J(z)\mathrm{d}z - A_i d_A. \tag{4b}$$

In order to assess the role of complex life cycles, we compare the above model to the analogous model with a simple life cycle that lacks an ontogenetic niche shift. The dynamics of resources and

5

consumers for this case are described by

$$\frac{\mathrm{d}R(z)}{\mathrm{d}t} = R(z)r\left(1 - \frac{R(z)}{K(z)}\right) - R(z)\sum_{i=1}^{n} a(z, x_i)N_i \qquad (5\text{a})$$

$$\frac{\mathrm{d}N_i}{\mathrm{d}t} = N_i c \int_{-\infty}^{+\infty} a(z, x_i)R(z)\,\mathrm{d}z - N_i d, \qquad (5\text{b})$$

where $K(z)$ and $a(z, x)$ are defined as in Equations (1) and (2), respectively.

Under the common assumption that resources have a much faster dynamics than consumers (Ackermann & Doebeli, 2004; MacArthur, 1972; Schoener, 1974), we show in Supplementary Information S1 and S2 that the consumer population dynamics for complex and simple life cycles can be re-formulated as Lotka-Volterra competition models, and these form the basis of our analysis. For the model with a complex life cycle, this results in a Lotka-Volterra model describing competition at two life-stages (see Equations S2) that, to the best of our knowledge, has not been presented before. For the model with a simple life cycle, the resulting model is equivalent to that derived by Ackermann & Doebeli (2004). Importantly, these models do not show the non-generic behavior known from the Lotka-Volterra competition model with Gaussian carrying capacity and competition functions (Barabás & Meszéna, 2009; Meszéna *et al.*, 2006; Szabó & Meszéna, 2006).

The system of Equations (5) has a globally stable equilibrium (Chesson, 1990; Haygood, 2002). In contrast, the consumer-resource model for complex life cycles given by Equations (3) and (4) can exhibit complex population dynamics, including limit cycles and alternative stable states (see Figure S1 and Schreiber & Rudolf (2008)). Since it is our aim to evaluate the role of complex life cycles in community assembly relative to communities of species with simple life cycles, we avoid the confounding effect of non-equilibrium population dynamics and restrict ourselves to parameter combinations that correspond to globally stable equilibria. Finally, for simplicity, we restrict ourselves to parameters such that all resources persist (i.e., the terms in brackets on the right-hand side of Equations S1 and S7 are positive). For the consequences of partial resource extinction on evolutionary diversification and coexistence see Abrams *et al.* (2008) and Abrams & Rueffler (2009).

Community assembly

We investigate community assembly of consumer species through two processes: gradual evolution and immigration. In the former case, we study the adaptive evolution of the niche position $\boldsymbol{x} = (x^J, x^A)$ of a founding species and all descendant species originating through recurrent mutation. In the latter case, we successively add immigrant species with randomly chosen niche positions $\boldsymbol{x}$. Hence, under both modes of community assembly, the number of coexisting species n is a variable quantity.

Community assembly through gradual evolution and immigration both rely on the probability that a newly-arrived mutant or immigrant is able to establish itself in a resident community, which encompasses whether the new type is favored by selection and can escape extinction due to demographic stochasticity while rare. For complex life cycles, we derive in Supplementary Information S3 that the *establishment probability* of a newly-arrived mutant or immigrant with phenotype $\boldsymbol{y} = (y^J, y^A)$ in a resident community consisting of n species with phenotypes $\boldsymbol{X} =$

$(\boldsymbol{x}_1, \ldots, \boldsymbol{x}_n)$ at population dynamical equilibrium is given by

$$p_{\text{est}}(\boldsymbol{y}, \boldsymbol{X}) = \frac{m(\boldsymbol{y}, \boldsymbol{X})}{m(\boldsymbol{y}, \boldsymbol{X}) + d_J} - \frac{d_A}{b(\boldsymbol{y}, \boldsymbol{X})}, \tag{6}$$

where $m(\boldsymbol{y}, \boldsymbol{X})$ and $b(\boldsymbol{y}, \boldsymbol{X})$ denote the maturation and birth rate, respectively. The expressions for these rates are given by Equations (S6a) and (S6b) in Supplementary Information S1. They encapsulate how the resident species affect the abundance of resources at the juvenile and adult stage, and how the niche position of the mutant or immigrant matches the available resources. We note that p_{est} is related to the basic reproductive ratio $R_0 = m/(m+d_J)*b/d_A$ (Schreiber & Rudolf, 2008) through the equality $p_{\text{est}} = d_A(R_0 - 1)/b$. Thus, a newly-arrived mutant or immigrant is able to establish itself if and only if $R_0 > 1$.

Gradual evolution. We study the gradual build-up of diversity giving rise to evolutionary trees as shown in Figure 2. We follow communities that originally consist of a single clonally reproducing species subject to mutations of small effect, affecting either the juvenile or adult trait. Mutations occur only once the resident community has reached its population dynamical equilibrium, resulting in a separation between the ecological and evolutionary time scales. Mutations are chosen randomly with probabilities proportional to the birth rate and adult population size of the parental species, and the establishment probability given by Equation (6). This accounts for the fact that mutations have a significant probability to go extinct due to demographic stochasticity. Mutants can either replace their parental type or coexist with it. In the latter case, an evolutionary lineage splits into two. We refer to this as an evolutionary branching event (Geritz *et al.*, 1998). Communities are saturated under gradual evolution once no further mutant with a positive establishment probability can be found. For simplicity, we refer to new lineages emerging through evolutionary branching as species, but fully acknowledge that in sexual populations speciation requires not only divergent natural selection but also the emergence of assortative mating between diverging lineages (for a review see Weissing *et al.*, 2011). This and similar methods (e.g., Champagnat *et al.*, 2006; Ito & Dieckmann, 2007; Pontarp & Petchey, 2018) are rooted in the derivation of the canonical equation of adaptive dynamics (Dieckmann & Law, 1996). For details see Supplementary Information S4 and S5.

Immigration. Community assembly through immigration is studied by successively adding new consumer species with randomly selected trait vectors to the community. We assume that immigration events are rare such that new species only appear once the resident community has reached its population dynamical equilibrium. The addition of a new species can result in the extinction of one or more resident species, which are then removed from the community. This process is iterated until the community is saturated, that is, until no further trait vector $\boldsymbol{y}$ with a positive establishment probability can be found. This mode of community assembly can also be interpreted as an evolutionary process in which mutations are not constrained to be of small effect. The full description of the immigration algorithm can be found Supplementary Information S5.

Results

To assess how complex life cycles affect community assembly we make several comparisons for the number of species in saturated communities (that is, communities to which no further species can be

added by, depending on the scenario, either mutations of small effect or immigration). We compare species richness for simple and complex life cycles first under gradual evolution and then under immigration. The results of these two modes of community assembly are then compared with each other.

To decouple the effect of life cycle complexity from effects due to differences in resource dynamics across stages, we assume identical intrinsic growth rates, $r_J = r = r_A$, and variances for the resource distributions, $\omega_J = \omega = \omega_A$. The total amount of resources available is scaled by the parameters k_J, k_A, and k (see Equations (1)). We focus on the case that $k_J = k_A = k = 1$, that is, juveniles, adults, and individuals with simple life cycles feed on the same amount of resources. This scenario is motivated by the hypothesis that the pronymph of the hemimetabolic insects evolved into the larval stage of the holometabola (Truman & Riddiford, 1999) with the novel larval stage being able to exploit a second set of resources. In other words, we study how adding a juvenile stage that can exploit a second set of resources to a simple life cycle alters community richness. In Supplementary Information S6 and S7 we furthermore present results for the case that species with simple life cycles feed on the same amount of resources as juveniles and adults of species with complex life cycles combined ($k = 2$), and for asymmetric juvenile and adults resource abundances ($k_J = 0.67$, $k_A = 1.33$ and $k_J = 1.33$, $k_A = 0.67$). These additional analyses confirm our findings.

Community assembly through gradual evolution and evolutionary branching

Studies of adaptive radiations in species with simple life cycles have shown that niche width is a crucial parameter determining species diversity, with narrower niche width allowing for more coexisting species, as narrower niches decrease the strength of inter-specific competition and thereby allow for a denser species packing (Ackermann & Doebeli, 2004; Bolnick, 2006; Dieckmann & Doebeli, 1999; Doebeli, 2011). Therefore, we vary juvenile and adult niche width: σ_J and σ_A can take the values 0.15, 0.3, 0.45, 0.6, 0.75. These values are combined in all possible ways, resulting in 25 combinations of niche widths. We then compare the evolved species richness of communities of species with complex life cycles with communities of species with simple life cycles for the case that $\sigma = \sigma_A$. This choice is made to keep the parameters for simple and complex life cycles as identical as possible. Since the birth rate is controlled by σ and σ_A for simple and complex life cycles, respectively, assuming $\sigma = \sigma_A$ is the most natural choice.

Figure 3 shows species richness averaged over ten simulation runs for both complex and simple life cycles. As expected, for simple life cycles species richness increases with decreasing niche width σ (compare horizontal black lines). A corresponding result holds for complex life cycles where species numbers increase with decreasing juvenile and decreasing adult niche width. For the juvenile niche width, this can be seen by comparing species richness for a fixed adult niche width (vertically arranged differently colored symbols). For the adult niche width, this can be seen by comparing the position of identical symbols horizontally for different adult niche width. For the case of very wide adult niche width ($\sigma_A = 0.75$) the latter pattern is less consistent.

The following observations can be made. First, species richness for complex life cycles is approximately equal to that for simple life cycles when the niche width of juveniles and adults is equal to that of individuals with a simple life cycle, $\sigma_J = \sigma_J = \sigma$ (see also green line Figure S5). Second, the fact that species with complex life cycles have two feeding niches can both favor and hinder diversification. If we compare species with complex life cycles that have one niche width identical to that of species with simple life cycles, but the other niche width narrower, then complex life cycles result in higher species richness. If, however, the other niche width is wider, then complex

life cycles tend to result in lower species richness. In conclusion, species richness resulting from an adaptive radiation in a clade with complex life cycles exceeds species richness in a clade with simple life cycles only if at least one of the life stages has a narrower niche width. Thus, complex life cycles do not *pe se* result in more species rich radiations.

This result may seem surprising given that species with complex life cycles forage on different sets of resources as juveniles and adults. It stems from the fact that communities of species with complex life cycles are arranged either diagonally or anti-diagonally in the two-dimensional trait space spanned by x_J and x_A, leaving large areas of the trait space unoccupied (Figure 4a). This can be understood as follows. Competition for resources selects for consumer trait values that decrease overlap in the spectrum of consumed resources (Abrams, 1986; Taper & Case, 1992). Species with complex life cycles compete at both the juvenile and adult life stage and, therefore, experience character displacement in the juvenile and adult traits simultaneously; two species that differ in both their juvenile and adult trait value compete less strongly with each other than species that differ at only one of their life stage. Such species pairs, when plotted in trait space, are arranged along either the diagonal or anti-diagonal. Whether gradual evolution results in a diagonal or anti-diagonal pattern is due to the stochasticity inherent in the mutation process. To understand the emergence of diagonal communities in more detail, we compute contour plots of the mutant establishment probability at various stages of an evolving community. Figure 5a-c illustrates the emergence of a diagonal community. For our choice of parameter values, the population contains more juvenile than adult individuals, resulting in evolutionary branching in the juvenile trait due to stronger competition (Figure 5a, b). Stochasticity in the sequence of mutations results in asymmetries in the divergence of the two species. Figure S3 in the Supplementary Information shows two examples how this can lead to the diagonal community shown in Figure 5c. In both cases, in a triangular community of three species the species that is not on the diagonal is prone to competitive exclusion because it competes with both species on the diagonal: with one at the juvenile stage and with the other at the adult stage (Figure S3b, f).

Community assembly through immigration

Figure 4c and 4d shows the number of species and their position in trait space for saturated communities resulting from immigration for complex and simple life cycles. For complex life cycles, immigration tends to result in communities in which all juvenile trait values and all adult trait values that are found in the evolved communities are paired with each other. This leads to a more complete filling of the trait space and communities that are arranged in a rectangle. As a consequence, with immigration, community richness with complex life cycles is approximately equal to community richness with simple life cycles to the power two (see orange line in Figure S5).

Immigration also tends to result in communities with clusters of similar species. This is due to long-lasting transients in the population dynamics of saturated communities. In this situation, fitness differences become extremely small so that clumps of similar species are pruned down only very slowly to single species. Similar patterns have also been reported by other authors (Fort *et al.*, 2009; Pigolotti *et al.*, 2010; Scheffer & van Nes, 2006). This cluster formation cannot occur under gradual evolution since, in our simulations, successful mutants always replace the parental type if they are not close to a branching point.

To assure that the extraordinary species richness with complex life cycles compared to simple life cycles in the immigration case is not due to our choice that species with complex life cycles have twice the amount of total resources available ($k = k_J = k_A = 1$), we show that the case

$k = k_J + k_A = 2$ does not produce qualitatively different results (Figures S9a and S5).

Gradual evolution versus immigration

Comparing the two modes of community assembly the main finding is that, for complex life cycles, communities assembled through immigration have a much higher species richness than communities assembled through gradual evolution. This difference is a result of the (anti-)diagonal pattern of communities assembled through gradual evolution, which leaves large part of the trait space unoccupied. In such communities, isolated fitness peaks appear away from the (anti-)diagonal. These peaks cannot be reached through gradual evolution but can be colonized by immigrants with suitable phenotypes, as illustrated in Figure 5d-f.

Discussion

We use mathematical modeling to investigate whether complex life cycles with an ontogentic niche shift allow for more diverse communities than simple life cycles without an ontogentic niche shift. To this end, we compare diversity in communities of consumer species with simple and complex life cycles that are the endpoint of two distinct assembly processes: gradual evolution with evolutionary branching resulting in adaptive radiations, and sequential immigration of randomly selected phenotypes.

We find that complex life cycles can both increase and decrease species richness in adaptive radiations resulting from gradual evolution when compared to species with simple life cycles. For an increase, it is necessary that at least one of the life stages has a narrower feeding niche than species with simple life cycles (Figure 3). This finding is related to what Débarre *et al.* (2014) refer to as *combinatorial effect*: the higher the dimension of the trait space, the more likely it becomes that conditions conducive to evolutionary diversification are met in one of the dimensions. The surprising finding that complex life cycles do not *per se* facilitate species richness under gradual evolution is due to such radiations only occupying the diagonal or anti-diagonal rather than the complete trait space. This arrangement results from character displacement acting on the juvenile and adult stage simultaneously. A related finding has recently been reported by ten Brink & Seehausen (2022), who show that adaptive radiations in adult traits of species with complex life cycles can be impeded if juveniles feed on a single resource of low productivity. This is because the ensuing strong competition among juveniles slows down maturation, resulting in a small adult population in which competition for resources is weak, which prevents competition driven adaptive radiations.

Our results are very different for communities assembled through sequential immigration. Here, the number of coexisting species with complex life cycles is approximately equal to the squared number of coexisting species with simple life cycles (Figure S5). This is evident from the rectangular arrangement of juvenile and adult trait values of species with complex life cycles compared to the linear arrangement of trait values in communities of species with simple life cycles (compare Figure 4c and d).

Comparing the two assembly processes we find that, for species with simple life cycles, gradual evolution and immigration lead to very similar communities (Figure 4b and d, ignoring cluster formation in the case of immigration) while this is distinctively not true for complex life cycles (Figure 4a and c). In the latter case, final communities assembled through immigration are stable against invasion of any mutant and, therefore, *globally stable* in the sense of Kremer & Klausmeier

(2017). In contrast, communities resulting from gradual evolution are not globally stable since they are uninvadable only by nearby mutants but can be invaded by immigrants reaching isolated fitness peaks away from the (anti-)diagonal (see Figure 5d-f). These two communities can be viewed as alternative stable states where the former is not reachable through gradual evolution starting with a single ancestral species. In contrast to our study, Rubin *et al.* (2021) find that also gradual evolution of complex phenotypes can lead to globally stable communities. Their finding is based on a Lotka-Volterra competition model where both the strength of competition and carrying capacity are functions of a multidimensional trait vector. Therefore, in our model, the unattainability of a globally stable community through gradual evolution is not a consequence of the two-dimensional trait space, but rather of competition occurring at two different life stages.

We note that an alternative interpretation of community assembly through sequential immigration is community assembly through evolution, but with mutations being unconstrained in both their step size and direction in trait space. In this sense, community assembly through immigration and through gradual evolution and evolutionary branching can be viewed as opposite extremes along a gradient of increasing mutational constraints.

Whether or not a community of species with complex life cycles can fill the entire two-dimensional trait space (as in Figure 4c) crucially also depends on whether the phenotype of the different ontogentic stages can evolve without being correlated with each other. This requires a high degree of modularity (*sensu* Wagner & Altenberg, 1996), which is what we assume in our model where juvenile and adult foraging traits vary independently. Several empirical studies suggest that such modularity is indeed widespread in organisms with complex life cycles. According to Yang (2001), the work of Truman & Riddiford (1999) shows that the juvenile and adult stages of the Holometabola have a higher degree of developmental modularity than the equivalent stages of the Hemimetabola. Similarly, recent studies based on gene-expression data (Wollenberg Valero *et al.*, 2017) and morphometrics (Sherratt *et al.*, 2017) suggest that the larval and adult stage in frogs are highly uncoupled.

Given the developmental modularity of holometabolic insects one can ask whether this is related to the extraordinary species richness in some families of insects (Mayhew, 2007). Indeed, based on the fossil record, Holometabola have been reported to exhibit a significantly higher diversification rates compared to the less modular Hemimetabola (Yang, 2001). The same conclusion was reached by Rainford *et al.* (2014) based on dated molecular phylogenies. Evidence that the uncoupling between larval and adult life stages affects radiations exists also for frogs. Bossuyt & Milinkovitch (2000) show that major adaptive radiations in ranid frogs result in diverse phenotypes at both the larval and adult stage. In line with these findings, it has been suggested that the ubiquity of complex life cycles among animals is due to the success of groups with such life cycles rather than to a high frequency of origin (Moran, 1994).

Our results are based on several simplifying assumptions, some of which we briefly discuss here. First, the population dynamical model for species with complex life cycles is known to allow for complex dynamics, including limit cycles and alternative stable states (Schreiber & Rudolf, 2008). Since our population dynamical model for species with simple life cycle always has a globally stable equilibrium and since we compare the results based on simple and complex life cycles with each other, we here excluded the confounding effect of non-equilibrium population dynamics. It would, however, be interesting to investigate whether the result that for complex life cycles communities assembled through gradual evolution are less species rich than communities assembled through immigration still holds true under fluctuating population dynamics. We suggest that this warrants a full blown study of its own. Second, in our complex life cycle model, juveniles and adults feed on mutually

exclusive sets of resources, which constitutes the most extreme form of ontogentic niche shift. This is an appropriate model for species with a complete metamorphosis such as holometabolic insects and anurans but also occurs in some fish and reptiles when individuals undergo a size-dependent habitat shift (for a review see Werner & Gilliam, 1984). In many other taxa, individuals include more prey types into their diet as they grow in body size (Werner & Gilliam, 1984; Wilson, 1975), resulting in a niche broadening rather than a niche shift. In this case, a larger species may simultaneously prey on and compete with a smaller species, a phenomenon known as life-history intraguild predation (e.g., Hin *et al.*, 2011; Polis *et al.*, 1989). Again, it will be interesting to see whether our results extend to species with complex life cycle but less abrupt niche shift.

In conclusion, our work shows that species richness can be significantly higher in communities of species with complex life cycles compared to communities of species with simple life cycles. Complex life cycles facilitate species rich communities if (i) the feeding niche is narrow in at least one of the ontogentic stages or (ii) the foraging related phenotypes in the two life stages can evolve independently and the mode of community assembly is not constrained to mutations of small effect. Our results are in qualitative agreement with empirical studies showing that larval and adult phenotypes can evolve independently in amphibians (Sherratt *et al.*, 2017; Wollenberg Valero *et al.*, 2017) and holometabolic insects (Truman & Riddiford, 1999), and that species diversity in radiations of holometabolic insects is higher than in radiations of hemimetabolic insects (Rainford *et al.*, 2014; Yang, 2001). We hope that these promising results will foster further interest in the role of complex life cycles for community composition and richness.

Acknowledgement

References

Abrams, P.A. (1986). Character displacement and niche shift analyzed using consumer-resource models of competition. *Theoretical Population Biology*, 29, 107–160.

Abrams, P.A. & Rueffler, C. (2009). Coexistence and limiting similarity of consumer species competing for a linear array of resources. *Ecology*, 90, 812–822.

Abrams, P.A., Rueffler, C. & Kim, G. (2008). Determinants of the strength of disruptive and/or divergent selection arising from resource competition. *Evolution*, 62, 1571–1586.

Ackermann, M. & Doebeli, M. (2004). Evolution of niche width and adaptive diversification. *Evolution*, 58, 2599–2612.

Allen, L.J.S. (2010). *An Introduction to Stochastic Processes with Applications to Biology*. Chapman and Hall/CRC.

Anaya-Rojas, J.M., Bassar, R.D., Potter, T., Blanchette, A., Callahan, S., Framstead, N., Reznick, D. & Travis, J. (2021). The evolution of size-dependent competitive interactions promotes species coexistence. *Journal of Animal Ecology*, 90, 2704–2717.

Barabás, G. & Meszéna, G. (2009). When the exception becomes the rule: The disappearance of limiting similarity in the lotka-volterra model. *Journal of Theoretical Biology*, 258, 89–94.

Bolnick, D.I. (2006). Multi-species outcomes in a common model of sympatric speciation. *Journal of Theoretical Biology*, 241, 734–744.

Bossuyt, F. & Milinkovitch, M.C. (2000). Convergent adaptive radiations in madagascan and asian ranid frogs reveal covariation between larval and adult traits. *Proceedings of the National Academy of Sciences of the United States of America*, 97, 6585–6590.

Champagnat, N., Ferrière, R. & Méléard, S. (2006). Unifying evolutionary dynamics: From individual stochastic processes to macroscopic models. *Theoretical Population Biology*, 69, 297–321.

Chesson, P. (1990). MacArthur's consumer-resource model. *Theoretical Population Biology*, 37, 26–38.

Claessen, D. & Dieckmann, U. (2002). Ontogenetic niche shifts and evolutionary branching in size-structured populations. *Evolutionary Ecology Research*, 4, 189–217.

Dieckmann, U. & Doebeli, M. (1999). On the origin of species by sympatric speciation. *Nature*, 400, 354–357.

Dieckmann, U. & Law, R. (1996). The dynamical theory of coevolution: a derivation from stochastic ecological processes. *Journal of Mathematical Biology*, 34, 579–612.

Doebeli, M. (2011). *Adaptive diversification*. Princeton University Press.

Débarre, F., Nuismer, S.L. & Doebeli, M. (2014). Multidimensional (co)evolutionary stability. *American Naturalist*, 184, 158–171.

Ebenman, B. (1992). Evolution in organisms that change their niches during the life cycle. *American Naturalist*, 139, 990–1021.

Eriksson, O. (2002). Ontogenetic niche shifts and their implications for recruitment in three clonal vaccinium shrubs: Vaccinium myrtillus, vaccinium vitis-idaea, and vaccinium oxycoccos. *Canadian Journal of Botany*, 80, 635–641.

Fort, H., Scheffer, M. & van Nes, E.H. (2009). The paradox of the clumps mathematically explained. *Theoretical Ecology*, 2, 171–176.

Geritz, S., Kisdi, E., Meszèna, G. & Metz, J.A. (1998). Evolutionarily singular strategies and the

adaptive growth and branching of the evolutionary tree. *Evolutionary Ecology*, 12, 35–57.

Hassell, M.P. & Comins, H.N. (1976). Discrete time models for two-species competition. *Theoretical Population Biology*, 9, 202–221.

Haygood, R. (2002). Coexistence in macarthur-style consumer–resource models. *Theoretical Population Biology*, 61, 215–223.

Hin, V., Schellekens, T., Persson, L. & de Roos, A.M. (2011). Coexistence of predator and prey in intraguild predation systems with ontogenetic niche shifts. *The American Naturalist*, 178, 701–714.

Istock, C.A. (1967). The evolution of complex life cycle phenomena: An ecological perspective. *Evolution*, 21, 592.

Ito, H.C. & Dieckmann, U. (2007). A new mechanism for recurrent adaptive radiations. *The American Naturalist*, 170.

Kremer, C.T. & Klausmeier, C.A. (2017). Species packing in eco-evolutionary models of seasonally fluctuating environments. *Ecology Letters*, 20, 1158–1168.

Landi, P., Vonesh, J.R. & Hui, C. (2018). Variability in life-history switch points across and within populations explained by adaptive dynamics. *Journal of the Royal Society Interface*, 15.

Lasky, J.R., Bachelot, B., Muscarella, R., Schwartz, N., Forero-Montaña, J., Nytch, C.J., Swenson, N.G., Thompson, J., Zimmerman, J.K. & Uriarte, M. (2015). Ontogenetic shifts in trait-mediated mechanisms of plant community assembly. *Ecology*, 96, 2157–2169.

Loreau, M. & Ebenhöh, W. (1994). Competitive exclusion and coexistence of species with complex life cycles. *Theoretical population biology*, 46, 58–77.

MacArthur, R. (1972). *Geographical Ecology (1st ed)*. Princeton University Press.

MacArthur, R. & Levins, R. (1967). The limiting similarity, convergence, and divergence of coexisting species. *American Naturalist*, 101, 377–385.

Mayhew, P.J. (2007). Why are there so many insect species? perspectives from fossils and phylogenies. *Biological Reviews*, 82, 425–454.

McPeek, M.A. (2022). *Coexistence in ecology : a mechanistic perspective*. Princeton University Press.

Meszéna, G., Gyllenberg, M., Pásztor, L. & Metz, J.A. (2006). Competitive exclusion and limiting similarity: A unified theory. *Theoretical Population Biology*, 69, 68–87.

Metz, H., Geritz, S.A.H., Meszéna, G., Jacobs, F.J.A. & van Heerwaarden, J.S. (1996). Adaptive dynamics: A geometrical study of the consequences of nearly faithful reproduction. In: *Stochastic and spatial structures of dynamical systems* (eds. van Strien, S. & Verduyn Lunel, S.). Proceedings of the Royal Dutch Academy of Science, North Holland, Dordrecht, pp. 183–231.

Miller, T.E. & Rudolf, V.H. (2011). Thinking inside the box: community-level consequences of stage-structured populations. *Trends in Ecology & Evolution*, 26, 457–466.

Moll, J.D. & Brown, J.S. (2008). Competition and coexistence with multiple life-history stages. *American Naturalist*, 171, 839–843.

Moran, N.A. (1994). Adaptation and constraint in the complex life cycles of animals. *Annual Review of Ecology and Systematics*, 25, 573–600.

Mougi, A. (2017). Persistence of a stage-structured food-web. *Scientific Reports*, 7, 1–5.

Nakazawa, T. (2011). Ontogenetic niche shift, food-web coupling, and alternative stable states.

Theoretical Ecology, 4, 479–494.

Nakazawa, T. (2015). Ontogenetic niche shifts matter in community ecology: a review and future perspectives. *Population Ecology*, 57, 347–354.

Parrish, J.A. & Bazzaz, F.A. (1985). Ontogenetic niche shifts in old-field annuals. *Ecology*, 66, 1296–1302.

Pigolotti, S., López, C., Hernández-García, E. & Andersen, K.H. (2010). How gaussian competition leads to lumpy or uniform species distributions. *Theoretical Ecology*, 3, 89–96.

Polis, G.A., Myers, C.A. & Holt, R.D. (1989). The ecology and evolution of intraguild predation: Potential competitors that eat each other. *Annual Review of Ecology and Systematics*, 20, 297–330.

Pontarp, M. & Petchey, O.L. (2018). Ecological opportunity and predator-prey interactions: linking eco-evolutionary processes and diversification in adaptive radiations. *Proceedings of the Royal Society B: Biological Sciences*, 285.

Rainford, J.L., Hofreiter, M., Nicholson, D.B. & Mayhew, P.J. (2014). Phylogenetic distribution of extant richness suggests metamorphosis is a key innovation driving diversification in insects. *PLOS ONE*, 9, e109085.

de Roos, A.M. (2021). Dynamic population stage structure due to juvenile-adult asymmetry stabilizes complex ecological communities. *Proceedings of the National Academy of Sciences of the United States of America*, 118, e2023709118.

de Roos, A.M. & Persson, L. (2013). *Population and community ecology of ontogenetic development.* Princeton University Press.

Rubin, I.N., Ispolatov, I. & Doebeli, M. (2021). Evolution to alternative levels of stable diversity leaves areas of niche space unexplored. *PLOS Computational Biology*, 17, e1008650.

Rudolf, V.H. & Eveland, L. (2021). Ontogenetic diversity buffers communities against consequences of species loss. *Journal of Animal Ecology*, 90, 1492–1504.

Rudolf, V.H. & Lafferty, K.D. (2011). Stage structure alters how complexity affects stability of ecological networks. *Ecology Letters*, 14, 75–79.

Scheffer, M. & van Nes, E.H. (2006). Self-organized similarity, the evolutionary emergence of groups of similar species. *Proceedings of the National Academy of Sciences of the United States of America*, 103, 6230–6235.

Schellekens, T., de Roos, A.M. & Persson, L. (2010). Ontogenetic diet shifts result in niche partitioning between two consumer species irrespective of competitive abilities. *American Naturalist*, 176, 625–637.

Schoener, T.W. (1974). Some methods for calculating competition coefficients from resource-utilization spectra. *The American Naturalist*, 108, 332–340.

Schreiber, S. & Rudolf, V.H. (2008). Crossing habitat boundaries: coupling dynamics of ecosystems through complex life cycles. *Ecology letters*, 11, 576–587.

Sherratt, E., Vidal-García, M., Anstis, M. & Keogh, J.S. (2017). Adult frogs and tadpoles have different macroevolutionary patterns across the australian continent. *Nature Ecology & Evolution*, 1, 1385–1391.

Szabó, P. & Meszéna, G. (2006). Limiting similarity revisited. *Oikos*, 112, 612–619.

Taper, M.L. & Case, T.J. (1992). Models of character displacement and the theoretical robustness of taxon cycles. *Evolution*, 46, 317–333.

ten Brink, H., de Roos, A.M. & Dieckmann, U. (2019). The evolutionary ecology of metamorphosis.

American Naturalist, 193, E116–E131.

ten Brink, H. & Seehausen, O. (2022). Competition among small individuals hinders adaptive radiation despite ecological opportunity. *Proceedings of the Royal Society B*, 289.

Truman, J.W. & Riddiford, L.M. (1999). The origins of insect metamorphosis. *Nature*, 401, 447–452.

Wagner, G.P. & Altenberg, L. (1996). Perspective: Complex adaptations and the evolution of evolvability. *Evolution*, 50, 967.

Weissing, F.J., Edelaar, P. & van Doorn, G.S. (2011). Adaptive speciation theory: A conceptual review. *Behavioral Ecology and Sociobiology*, 65, 461–480.

Werner, E.E. (1988). Size, scaling, and the evolution of complex life cycles. In: *Size-Structured Populations* (eds. Ebenman, B. & Persson, L.). Springer, Berlin, Heidelberg, pp. 60–81.

Werner, E.E. & Gilliam, J.F. (1984). The ontogenetic niche and species interactions in size-structured populations. *Annual Review of Ecology and Systematics*, 15, 393–425.

Wilbur, H.M. (1980). Complex life cycles. *Annual Review of Ecology and Systematics*, 11, 67–93.

Wilson, D.S. (1975). The adequacy of body size as a niche difference. *The American Naturalist*, 109, 769–784.

Wollenberg Valero, K.C., Garcia-Porta, J., Rodríguez, A., Arias, M., Shah, A., Randrianiaina, R.D., Brown, J.L., Glaw, F., Amat, F., Künzel, S., Metzler, D., Isokpehi, R.D. & Vences, M. (2017). Transcriptomic and macroevolutionary evidence for phenotypic uncoupling between frog life history phases. *Nature Communications*, 8, 1–9.

Wollrab, S., Roos, A.M.D. & Diehl, S. (2013). Ontogenetic diet shifts promote predator-mediated coexistence. *Ecology*, 94, 2886–2897.

Yang, A.S. (2001). Modularity, evolvability, and adaptive radiations: a comparison of the hemi- and holometabolous insects. *Evolution & Development*, 3, 59–72.
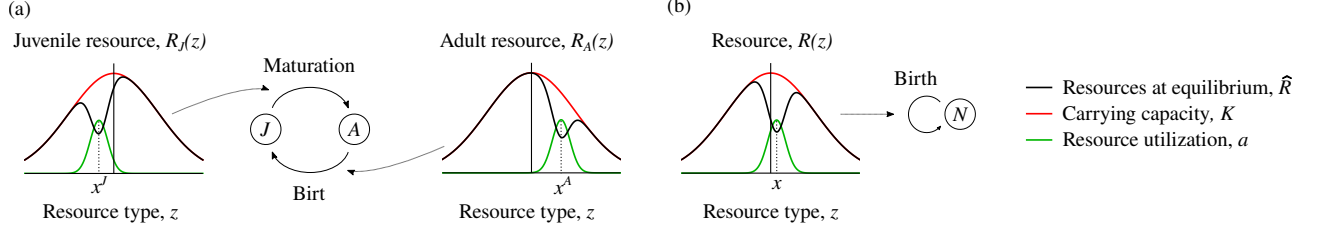
Figure 1: (a) Schematic of the population dynamical model for complex life cycles. Juvenile individuals J mature into adult individuals A, which, in turn, give birth to new juveniles. Juveniles and adults feed on resources $R_J(z)$ and $R_A(z)$, respectively, and the rates at which these resources are consumed determines the maturation and birth rate. The abundance of resources in the absence of consumers is determined by the stage-specific carrying capacity functions $K_J(z)$ and $K_A(z)$ (red lines). Juveniles and adults feed on the resources with feeding efficiencies given by the Gaussian functions $a_J(z, x^J)$ and $a_A(z, x^A)$ (green lines), leading to the depletion of resources in the neighborhood of the consumer trait values and to the equilibrium resource distributions $\hat{R}_J$ and $\hat{R}_A$ (black lines). b) Consumer individuals N with simple life cycle feed on a single resource distribution, and their rate of resource consumption determines the birth rate.
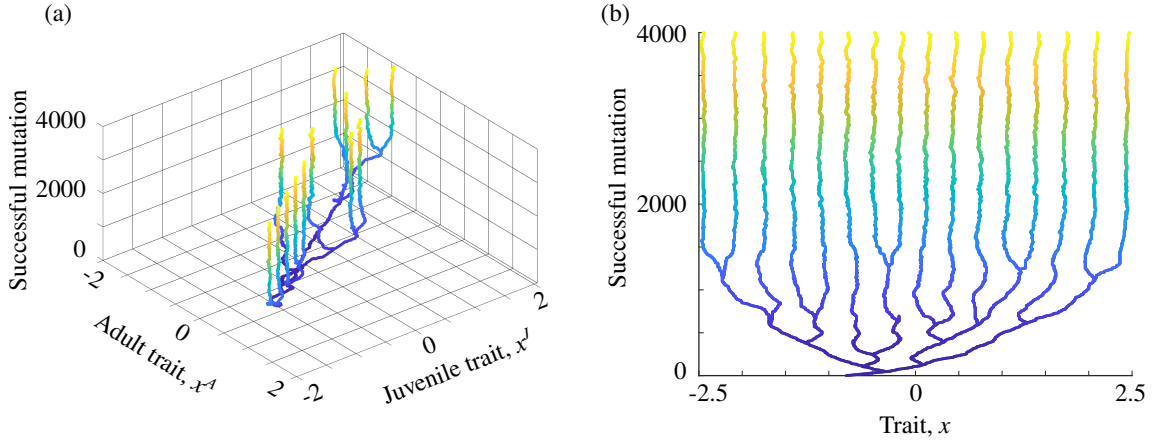

Figure 2: Simulated evolutionary trees resulting from gradual evolution for (a) complex and (b) simple life cycles. For complex life cycles, gradual evolution leads to diagonal community, leaving large parts of the trait space unoccupied. Time, measured in number of successful mutations, is shown on the vertical axes and color changes from dark to light as time proceeds. The dots in Figure 4a, b correspond to the end points of these simulated trees. If not stated otherwise, all figures are based on the following parameter values: $r = 0.4$, $\omega = 1.5$, $k_J = k_A = k = 1$, $d_J = 1 = d_A$, $c_J = 1.5$, $c_A = c = 6$. Parameters specific to this figure are (a) $\sigma_J = 0.15 = \sigma_A$, (b) $\sigma = 0.15$.
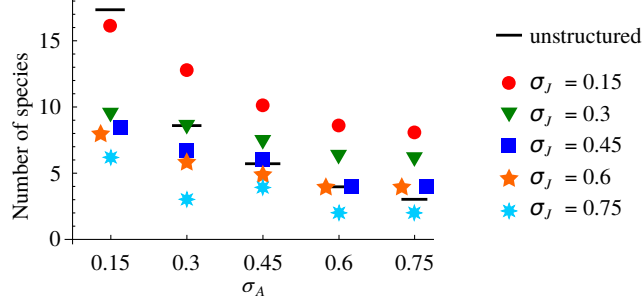
Figure 3: Number of coexisting species resulting from gradual evolution averaged over ten simulation runs. For complex life-cycles, results are shown for 25 combinations of five adult (σ_A, horizontal axis) and five juvenile (σ_J, colored symbols) niche widths. Results for simple life cycles are given by the black lines, where the niche width σ is equal to the values for σ_A along the x-axis. For the exact numerical values see Figure S4. Parameters as in Figure 2.
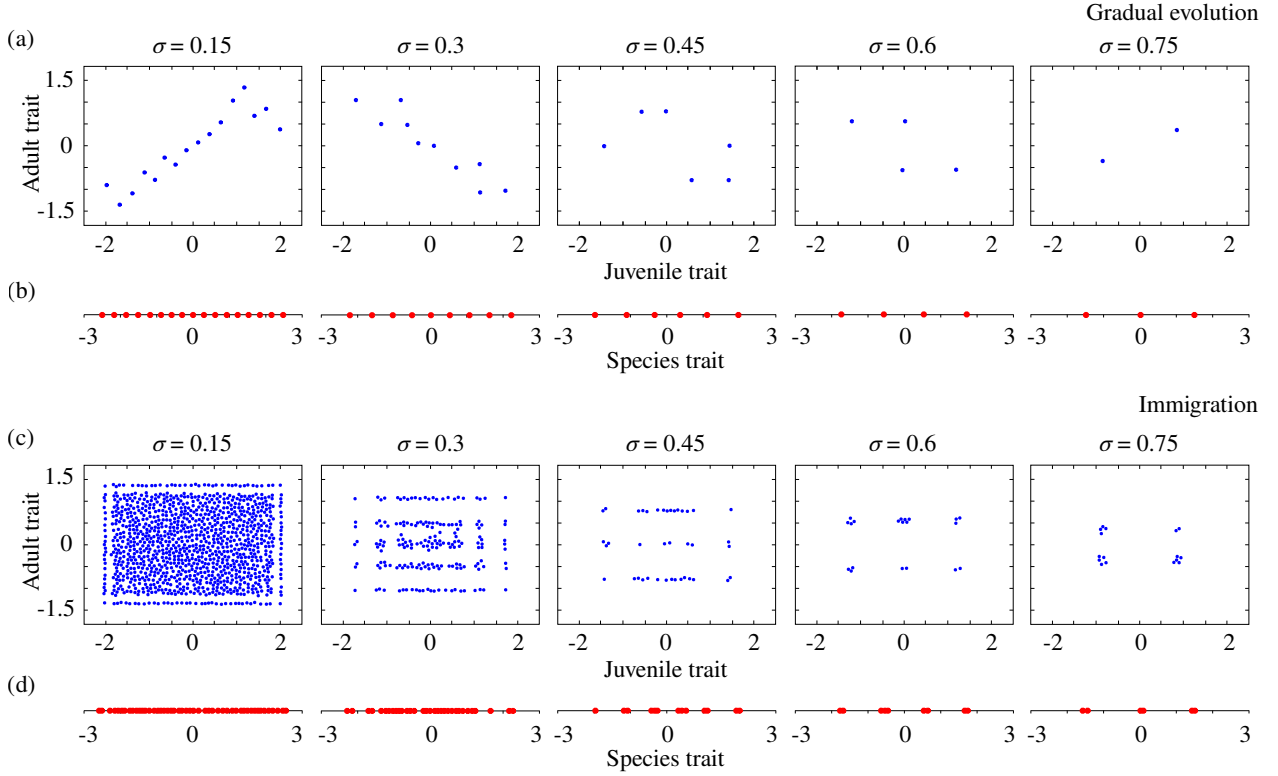

Figure 4: Composition of saturated communities resulting from (a, b) gradual evolution and (c, d) immigration for five different values of the niche width σ. For complex life cycles we assume an equal niche width for juvenile and adult individuals ($\sigma_J = \sigma = \sigma_A$). Coexisting species are represented by dots at their position in trait space, which is two-dimensional for complex (a, c) and one-dimensional for simple life cycles (b, d). Parameters as in Figure 2.
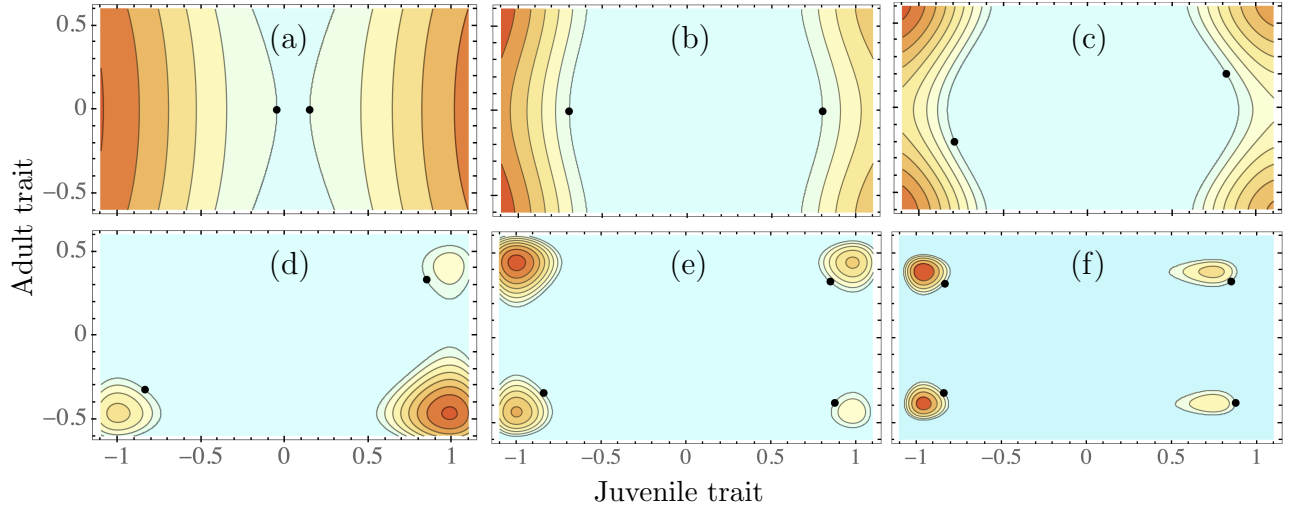
Figure 5: The emergence of a diagonal community through gradual evolution and of a rectangular community through immigration for $\sigma_J = 0.75 = \sigma_A$ (compare most right panels in Figure 4a, c). Black dots show the trait vectors of resident species. Contour lines indicate the establishment probability p_{est} of possible mutants with warmer colors indicating higher values. Residents are always located at the zero-contour line. (a) Two resident species shortly after evolutionary branching in the juvenile trait. Selection favors further character displacement in the juvenile trait. (b) Two resident species after a long period of divergence in the juvenile trait. Selection continues to favor character displacement in the juvenile trait but now also specialization in the adult trait. (c) Two resident species that have diverged in both their juvenile and adult trait values. The emergence of this diagonal community is analyzed in more detail in Figure S3. Selection favors further character displacement in both the juvenile and adult trait. (d) Two resident species close to local fitness peaks. A further fitness peak has appeared away from the diagonal that cannot be reached through gradual evolution. A corresponding fitness peak in the top-left is missing due to asymmetries in the resident's trait vectors. (e) An immigrant species occupying the bottom-right fitness peak has been added to the community. This causes the emergence of a new fitness peak in the top-left of the trait space. (f) An immigrant species occupying the top-left fitness peak has been added to the community. Each of the four coexisting species experiences selection towards a different local fitness peak. Numerical simulations show that in this situation the population dynamics becomes exceedingly slow. The time scale separation breaks down and clouds of similar species coexisting at each fitness peak can emerge (see most right panel in Figure 4c). Contour lines correspond to increasingly lower differences in p_{est} (0.02 in (a) to 0.00002 in (f)). Parameters as in Figure 2.

Supplementary Information

S1   Population dynamics for species with complex life cycles

In this section, we show that the population dynamics given by Eq. (4) can be rewritten in a form akin to a Lotka-Volterra competition model that takes ontogentic diet shift into account. Under the common assumption that resources have a much faster dynamics than consumers (Ackermann & Doebeli, 2004; Schoener, 1974), the dynamics of the resource densities given by Eqs. (3) reach a quasi-equilibrium given by

$$\hat{R}_J(z, \boldsymbol{X}^J, \boldsymbol{J}) = K(z) \left[1 - \frac{\sum_{i=1}^{n} a(z, x_i^J) J_i}{r} \right], \tag{S1a}$$

$$\hat{R}_A(z, \boldsymbol{X}^A, \boldsymbol{A}) = K(z) \left[1 - \frac{\sum_{i=1}^{n} a(z, x_i^A) A_i}{r} \right], \tag{S1b}$$

where $\boldsymbol{X}^J = (x_1^J, \ldots, x_n^J)$ and $\boldsymbol{X}^A = (x_1^A, \ldots, x_n^A)$ are, respectively, the vectors of juvenile and adult trait values of all species present in the population, and $\boldsymbol{J} = (J_1, \ldots, J_n)$ and $\boldsymbol{A} = (A_1, \ldots, A_n)$ are the vectors of corresponding population densities. Inserting these quasi-equilibrium resource densities into Eqs. (4a) and (4b), respectively, and solving the integrals results in

$$\frac{\mathrm{d}J_i}{\mathrm{d}t} = b(x_i^A, \boldsymbol{X}^A, \boldsymbol{A}) A_i - m(x_i^J, \boldsymbol{X}^J, \boldsymbol{J}) J_i - d_J J_i, \tag{S2a}$$

$$\frac{\mathrm{d}A_i}{\mathrm{d}t} = m(x_i^J, \boldsymbol{X}^J, \boldsymbol{J}) J_i - d_A A_i, \tag{S2b}$$

where

$$m(x_i^J, \boldsymbol{X}^J, \boldsymbol{J}) = m_0(x_i^J) \left(1 - \sum_{j=1}^{n} \alpha_J(x_i^J, x_j^J) J_j \right), \tag{S3a}$$

$$b(x_i^A, \boldsymbol{X}^A, \boldsymbol{A}) = b_0(x_i^A) \left(1 - \sum_{j=1}^{n} \alpha_A(x_i^A, x_j^A) A_j \right) \tag{S3b}$$

are the species specific maturation and birth rate, respectively. Here, the vectors $\boldsymbol{X}^J = (x_1^J, \ldots, x_n^J)$ and $\boldsymbol{X}^A = (x_1^A, \ldots, x_n^A)$ collect the juvenile and adult trait values, respectively, of all species present in the population and $\boldsymbol{J} = (J_1, \ldots, J_n)$ and $\boldsymbol{A} = (A_1, \ldots, A_n)$ collect the corresponding population densities. Furthermore, $m_0(x_i^J)$ and $b_0(x_i^A)$ are the species-specific intrinsic maturation and birth rates, respectively, that describe the maximum rate of maturation and birth in the absence of

competition. They are given by

$$m_0(x_i^J) = c_J \frac{\omega k}{\sqrt{\sigma_J^2 + \omega^2}} \exp\left[-\frac{\left(x_i^J\right)^2}{2\left(\sigma_J^2 + \omega^2\right)}\right], \tag{S4a}$$

$$b_0(x_i^A) = c_A \frac{\omega k}{\sqrt{\sigma_A^2 + \omega^2}} \exp\left[-\frac{\left(x_i^A\right)^2}{2\left(\sigma_A^2 + \omega^2\right)}\right]. \tag{S4b}$$

Finally, $\alpha_J(x_i^J, x_j^J)$ and $\alpha_A(x_i^A, x_j^A)$ are the competition coefficients describing the competitive effect of species j on species i in the juvenile and adult stage, respectively, and are given by

$$\alpha_J(x_i^J, x_j^J) = \frac{1}{\sqrt{2\pi}r} \sqrt{\frac{\sigma_J^2 + \omega^2}{\sigma_J^2 + 2\omega^2}} \exp\left[-\frac{\omega^2 \left(x_i^J - x_j^J\right)^2 + \sigma_J^2\left(\left(x_i^J\right)^2 + \left(x_j^J\right)^2\right)}{2\sigma_J^2\left(\sigma_J^2 + 2\omega^2\right)} + \frac{\left(x_i^J\right)^2}{2\left(\sigma_J^2 + \omega^2\right)}\right], \tag{S5a}$$

$$\alpha_A(x_i^A, x_j^A) = \frac{1}{\sqrt{2\pi}r} \sqrt{\frac{\sigma_A^2 + \omega^2}{\sigma_A^2 + 2\omega^2}} \exp\left[-\frac{\omega^2 \left(x_i^A - x_j^A\right)^2 + \sigma_A^2\left(\left(x_i^A\right)^2 + \left(x_j^A\right)^2\right)}{2\sigma_A^2\left(\sigma_A^2 + 2\omega^2\right)} + \frac{\left(x_i^A\right)^2}{2\left(\sigma_A^2 + \omega^2\right)}\right]. \tag{S5b}$$

In Supplementary Information S3, we compute the establishment probability p_{est} of newly-arrived mutants. It is calculated under the assumption that the resident consumer species have reached their juvenile and adult equilibrium abundances ($\hat{J}_j$ and $\hat{A}_j$). These are fully determined by $\boldsymbol{X}$, the collection of trait vectors of all species present in the community. Therefore, the explicit dependency of the functions m and b on the juvenile and adult densities can be dropped, and Eqs. (S3) becomes

$$m(x_i^J, \boldsymbol{X}) = m_0(x_i^J)\left(1 - \sum_{j=1}^n \alpha_J(x_i^J, x_j^J)\hat{J}_j\right), \tag{S6a}$$

$$b(x_i^A, \boldsymbol{X}) = b_0(x_i^A)\left(1 - \sum_{j=1}^n \alpha_A(x_i^A, x_j^A)\hat{A}_j\right). \tag{S6b}$$

S2   Population dynamics for species with simple life cycles

In this section, we show that the population dynamics given by Eq. (5) can be rewritten as a classic Lotka-Volterra competition model. As in the model for species with complex life cycles, we assume that the resources have much faster dynamics than the consumers so that the dynamics of the resource densities given by Eq. (5a) reach a quasi-equilibrium given by

$$\hat{R}(z, \boldsymbol{X}, \boldsymbol{N}) = K(z)\left[1 - \frac{\sum_{i=1}^n a(z, x_i)N_i}{r}\right], \tag{S7}$$

where $\boldsymbol{X} = (x_1, \ldots, x_n)$ is the vector of trait values of all species present in the population and $\boldsymbol{N} = (N_1, \ldots, N_n)$ the vector of corresponding population densities.

Inserting this equation into Eq. (5b) and solving the integral results in

$$\frac{\mathrm{d}N_i}{\mathrm{d}t} = b(x_i, \boldsymbol{X}, \boldsymbol{N})N_i - dN_i, \qquad (S8)$$

where

$$b(x_i, \boldsymbol{X}, \boldsymbol{N}) = b_0(x_i) \left(1 - \sum_{j=1}^{n} \alpha(x_i, x_j)N_j \right), \qquad (S9)$$

is the species specific birth rate. Here, $b_0(x_i)$ is the species-specific intrinsic birth rate that describes the maximum birth rate in the absence of competition. It is given by

$$b_0(x_i) = c\frac{\omega k}{\sqrt{\sigma^2 + \omega^2}} \exp\left[-\frac{x_i^2}{2\left(\sigma^2 + \omega^2\right)} \right]. \qquad (S10)$$

Furthermore,

$$\alpha(x_i, x_j) = \frac{1}{\sqrt{2\pi}r} \sqrt{\frac{\sigma^2 + \omega^2}{\sigma^2 + 2\omega^2}} \exp\left[-\frac{\omega^2 \left(x_i - x_j\right)^2 + \sigma^2 x_i^2 + \sigma^2 x_j^2}{2\sigma^2 \left(\sigma^2 + 2\omega^2\right)} + \frac{x_i^2}{2\left(\sigma^2 + \omega^2\right)} \right] \qquad (S11)$$

is the competition coefficient describing the competitive effect of species j on species i.

In Supplementary Information S3, we compute the establishment probability p_{est} of newly-arrived mutants, which is calculated under the assumption that the resident consumer species have reached their equilibrium abundances $\hat{N}_j$. These are fully determined by $\boldsymbol{X}$, the collection of traits of all species present in the community. Therefore, the explicit dependency of the function b on the population densities can be dropped, and Eq. (S9) becomes

$$b(x_i, \boldsymbol{X}) = b_0(x_i) \left(1 - \sum_{j=1}^{n} \alpha(x_i, x_j)\hat{N}_j \right). \qquad (S12)$$

S3   Derivation of the establishment probability for complex life cycles

For a beneficial mutation occurring in a single individual to increase in frequency and establish itself it is necessary to successfully escape demographic stochasticity. For simple life cycles, the probability to do so in a large population of residents equals 0 if $b \leq d$ and $1 - d/b$ if $b > d$ (e.g., Allen, 2010), where b is given by Eq. (S12). Here, we derive the analogous expression for complex life cycles.

We consider a community of resident species with trait vectors $\boldsymbol{x}_i$ collected in $\boldsymbol{X}$ that has settled on a unique asymptotically stable fixed point equilibrium. If we furthermore assume that the juvenile and adult population sizes of all resident species are large, then the maturation rate m and birth rate b of the mutant sub-population during its establishment phase in which it is sensitive to demographic stochasticity are approximately constant and given by Eq. (S6). The dynamics of the mutant sub-population can thus be described as a continuous time Markov process and the waiting

times until maturation, death as a juvenile, death as an adult and birth for a mutant individual are exponentially distributed and given by

$$q_m(t) = m e^{-mt} \Theta(t), \tag{S13a}$$

$$q_{d_J}(t) = d_J e^{-d_J t} \Theta(t), \tag{S13b}$$

$$q_{d_A}(t) = d_A e^{-d_A t} \Theta(t), \tag{S13c}$$

$$q_b(t) = b e^{-bt} \Theta(t), \tag{S13d}$$

where we dropped for simplicity the explicit dependency of b and m on the traits. Here, $\Theta(t)$ is Heaviside step function (i.e., $\Theta(t) = 0$ for $t < 0$, and $\Theta(t) = 1$ for $t \geq 0$). The four events are statistically independent. Thus, the probability that a mutant individual produces progeny is the product of the probability that it matures, M, and the probability that it gives birth, B. We first calculate M. Let T_M be a random variable defined as

$$T_M = T_{d_J} - T_m, \tag{S14}$$

where T_m and T_{d_J} are, respectively, the random variables for the waiting time for a juvenile to mature and for a juvenile to die. Since T_m and T_{d_J} are defined in $(0, \infty)$ the random variable T_M is defined in $(-\infty, +\infty)$. The probability M for a juvenile to mature can then be written as

$$M = \mathbb{P}\left(T_{d_J} > T_m\right) = \mathbb{P}\left(T_{d_J} - T_m > 0\right) = \mathbb{P}\left(T_M > 0\right). \tag{S15}$$

Since the probability density function of the sum of two random variables is given by the convolution of their respective probability density functions, the probability density function q_M of the random variable T_M computes as

$$q_M(t) = \int_{-\infty}^{+\infty} q_{d_J}(t + \tau) \, q_m(\tau) \, \mathrm{d}\tau = \frac{m \, d_J}{m + d_J} \left[e^{-d_J t} \, \Theta(t) + e^{-mt} \, \Theta(-t) \right]. \tag{S16}$$

The probability of maturation M can then be calculated as

$$M = \mathbb{P}\left(T_M > 0\right) = \int_0^{+\infty} q_M(t) \, \mathrm{d}t = \frac{m}{m + d_J}. \tag{S17}$$

The probability B for an adult individual to give birth can be calculated analogously and equals

$$B = \frac{b}{b + d_A}. \tag{S18}$$

Due to the memorylessness of the involved stochastic processes, the probability for an adult individual to give birth n times *given* that it has already given birth $n - 1$ times, equals the probability for an adult to give birth $n - 1$ times *given* that it has already given birth $n - 2$ times. Thus, the generation of new individuals as a result of reproduction is a Bernoulli trial. Hence, the probability for an adult individual to reproduce *exactly* n times is

$$Q(n) = (1 - B) \, B^n. \tag{S19}$$

Here, B^n corresponds to n successful birth events and $(1 - B)$ corresponds to the $(n + 1)$th unsuccessful attempt where the individual dies before giving birth.

For the next step in the derivation of the establishment probability it is useful to first note that the expected lifetime number of offspring (or basic reproductive ratio) of a newly-born individual is given by

$$R_0 = \langle n \rangle = M \sum_{n=0}^{\infty} n \, Q(n) = M \frac{B}{1-B} = \frac{m}{m+d_J} \frac{b}{d_A}. \tag{S20}$$

Let p_{ex} be the probability that a lineage starting with a single mutant goes extinct. This happens if the mutant does not mature or it does mature but that all lineages resulting from successful reproduction go extinct. Thus

$$p_{\mathrm{ex}} = 1 - M + M \sum_{n=0}^{\infty} Q(n) \, p_{\mathrm{ex}}^n = 1 - M + M \frac{1-B}{1-B \, p_{\mathrm{ex}}}. \tag{S21}$$

Solving this equation for p_{ex} results in

$$p_{\mathrm{ex}} = \frac{1}{2B} \big[1 + B(1-M) \pm |B(1+M) - 1| \big]. \tag{S22}$$

To find an interpretable expressions for p_{ex} we distinguish two cases depending on whether $B(1+M) - 1$ is positive or negative and note that

$$B(1+M) - 1 \gtreqless 0 \iff R_0 \gtreqless 1.$$

We start with the solution of p_{ex} corresponding to the plus-sign on the right-hand side of Eq. (S22). Then, simplifying the right-hand side, we obtain $p_{\mathrm{ex}} > 1$ for $R_0 < 1$ and $p_{\mathrm{ex}} = 1$ for $R_0 \geq 1$, even as B and M approach 1. Both results are biologically meaningless. For the solution of p_{ex} corresponding to the minus-sign on the right-hand side of Eq. (S22) we obtain

$$p_{\mathrm{ex}} = \begin{cases} 1 & \text{if } R_0 \leq 1, \\[2mm] \frac{1}{B} - M & \text{if } R_0 > 1, \end{cases} \tag{S23}$$

which is indeed the relevant solution. Thus, the establishment probability $p_{\mathrm{est}} = 1 - p_{\mathrm{ex}}$ is given by

$$p_{\mathrm{est}} = \begin{cases} 0 & \text{if } R_0 \leq 1, \\[2mm] M - \frac{1-B}{B} & \text{if } R_0 > 1. \end{cases} \tag{S24}$$

Using the definitions for M and B the probability for a mutant with $R_0 > 1$ to successfully establish itself equals

$$p_{\mathrm{est}} = \frac{m}{m+d_J} - \frac{d_A}{b} = \frac{d_A}{b} (R_0 - 1). \tag{S25}$$

The term $m/(m+d_J)$ is the probability that a newly-born juvenile reaches the adult stage, a prerequisite for reproduction. Notice that, in the limit of very fast maturation ($m \to \infty$), this term approaches 1 since all newly-born individuals mature. In this case, the life cycle reduces to the simple version given by Eq. (5a) and $p_{\mathrm{est}} = 1 - d_A/b$. This is indeed the establishment probability in a simple birth-death process (e.g., Allen, 2010), and our expression is its natural generalization.

S4 Gradual evolution

We study the gradual build-up of diversity by investigating the fate of recurrent mutations. Following the adaptive dynamics approximation (Dieckmann & Law, 1996; Geritz *et al.*, 1998; Metz *et al.*, 1996), we assume that mutations are rare and occur in a large clonal population. The first assumption ensures that new mutations arise only after all resident species have reached their population dynamical equilibrium, resulting in a separation between fast ecological and slow evolutionary time scale. With the assumption of large population size we exclude the possibility that resident species go extinct via demographic stochasticity. In contrast, the establishment of new mutations is subject to demographic stochasticity such that even beneficial mutations have a significant risk of going extinct. Together, these assumptions result in evolution proceeding as a trait substitution sequence that can be described as a directed random walk driven by mutation and selection (Champagnat *et al.*, 2006; Dieckmann & Law, 1996; Metz *et al.*, 1996). Importantly, this process can result in the gradual build-up of diversity, which occurs whenever a successful mutant does not replace its progenitor but is able coexist with it in a protected polymorphism. In the following, we describe an efficient computational simulation algorithm to study the evolutionary dynamics. A step-by-step description is given in Supplementary Information S5.

Following Dieckmann & Law (1996) and Champagnat *et al.* (2006), the rate that a mutant with trait vector $\boldsymbol{y}_i$ invades and replaces its parental species with trait vector $\boldsymbol{x}_i$ in a n-species community with trait vectors collected in $\boldsymbol{X}$ is given by

$$g(\boldsymbol{y}_i, \boldsymbol{X}) = \mu \, \hat{A}_i \, b(\boldsymbol{x}_i, \boldsymbol{X}) \, p_{\text{est}}(\boldsymbol{y}_i, \boldsymbol{X}). \tag{S26}$$

Here, μ denotes the probability that a newborn individual carries a mutation, $\hat{A}_i$ is the equilibrium adult population size of species i and $b(\boldsymbol{x}_i, \boldsymbol{X})$ its *per-capita* birth rate as defined in Eq. (S6b). Finally, $p_{\text{est}}(\boldsymbol{y}_i, \boldsymbol{X})$ denotes the probability that a mutant with trait vector $\boldsymbol{y}_i$ escapes extinction due to demographic stochasticity and successfully establishes itself in the population. It is given by

$$p_{\text{est}}(\boldsymbol{y}_i, \boldsymbol{X}) = \frac{m(\boldsymbol{y}_i, \boldsymbol{X})}{m(\boldsymbol{y}_i, \boldsymbol{X}) + d_J} - \frac{d_A}{b(\boldsymbol{y}_i, \boldsymbol{X})}, \tag{S27}$$

were $m(\boldsymbol{y}_i, \boldsymbol{X})$ is the maturation rate of the mutant as defined in Eq. (S6a). The formal derivation of p_{est} is given in Supplementary Information S3.

We assume that the juvenile and adult traits are uncorrelated and that mutations have a fixed step size $\epsilon = 0.01$. Furthermore, the probability μ that an offspring carries a mutation is small ($\mu \ll 1$) and, therefore, the probability μ^2 to carry two mutations is negligible. Then, each resident species with trait vector $\boldsymbol{x}_i$ can give rise to four possible mutants: $\boldsymbol{y}_i = (x_i^J - \epsilon, x_i^A)$, $\boldsymbol{y}_i = (x_i^J + \epsilon, x_i^A)$, $\boldsymbol{y}_i = (x_i^J, x_i^A - \epsilon)$, and $\boldsymbol{y}_i = (x_i^J, x_i^A + \epsilon)$. Both traits mutate with equal probability (though they do not, in general, establish with equal probability) and mutations that increase a trait value are as likely as mutations that decrease a trait value (mutations are isotropic). Under these assumptions, the probability that a particular trait vector $\boldsymbol{y}_i$ is chosen as the next successful mutant is given by $g(\boldsymbol{y}_i, \boldsymbol{X})/\sum_{\{\boldsymbol{y}\}} g(\boldsymbol{y}, \boldsymbol{X})$, where the summation runs over all $4n$ ($2n$ for simple life cycles) possible mutants that can appear in an n-species community. We model evolution as occurring in a continuous time. In this sense, only one mutation can occur at a time, as no two events can occur simultaneously in a continuous time frame. However, in our computational algorithm, we measure time in units of successful mutations T. A consequence of this choice is that, in general, the physical time passed between T and $T + 1$ is different from the physical time passed between $T + 1$ and $T + 2$.

A mutant $\boldsymbol{y}_i$ that successfully establishes itself generally replaces its progenitor $\boldsymbol{x}_i$. This is the case when $p_{\text{est}}(\boldsymbol{y}_i, \boldsymbol{X}) > 0$ and $p_{\text{est}}(\boldsymbol{x}_i, \boldsymbol{Y}) = 0$, where $\boldsymbol{Y} = (\boldsymbol{x}_1, \ldots, \boldsymbol{y}_i, \ldots, \boldsymbol{x}_n)$. In this case, the resident population with trait vector $\boldsymbol{x}_i$ is removed from the community and replaced by the mutant with trait vector $\boldsymbol{y}_i$. An important exception are mutants that originate from a resident species with a trait value close to an evolutionary branching point. These are points in trait space that are attractors of a trait substitution sequence and, simultaneously, local minima of the fitness landscape (Geritz *et al.*, 1998). It is then possible that a mutant establishes itself and coexists with its progenitor so that the number of species increases by one. Species $\boldsymbol{y}_i$ is then added to the community. This is the case when $p_{\text{est}}(\boldsymbol{y}_i, \boldsymbol{X}) > 0$ and $p_{\text{est}}(\boldsymbol{x}_i, \boldsymbol{Y}) > 0$. Evolution according to this algorithm results in evolutionary trees as shown in Figure 2. For an illustration of the algorithm, see Figure S2.

S5   The simulation algorithms

Community assembly through gradual evolution

We use stochastic computer simulations to study community assembly through gradual adaptive evolution. The simulation algorithm is programmed in C++ and works as follows:

(1) Simulations are started with a monomorphic population with trait vector $(x^J, x^A) = (-0.3, 0.1)$ for complex life cycles and $x = 0.1$ for simple life cycles.

(2) Numerically solve Eq. (S2) in case of simple life cycles and Eq. (S8) in case of complex life cycles using Euler's forward method with a time increment of $t = 0.1$. We consider the system to have reached equilibrium once the difference between the density of every species present in the population before and after an iteration of the population dynamics is less than 10^{-7} or after a maximum of 10^5 iterations has been reached.

(3) Delete any lineage with a total density $(J + A)$ less than the extinction threshold, set to 0.004.

(4) For each of the n species $\boldsymbol{x}_i$ present in the population, determine the four mutant trait vectors $\boldsymbol{y}_i = (x_i^J - \epsilon, x_i^A)$, $\boldsymbol{y}_i = (x_i^J + \epsilon, x_i^A)$, $\boldsymbol{y}_i = (x_i^J, x_i^A - \epsilon)$, and $\boldsymbol{y}_i = (x_i^J, x_i^A + \epsilon)$, where $\epsilon = 0.01$, resulting in $4n$ mutants ($2n$ for simple life cycles).

(5) Assign to each possible mutant the probability $g(\boldsymbol{y}_i, \boldsymbol{X})/\sum_{\{\boldsymbol{y}\}} g(\boldsymbol{y}, \boldsymbol{X})$ for it to be the next mutant successfully invading the community $\boldsymbol{X}$, where the summation runs over all $4n$ possible mutants ($2n$ for simple life cycles). The function $g(\boldsymbol{y}_i, \boldsymbol{X})$ is given by Eq. S26. Herein, p_{est} is given by Eq. (S24) in case complex life cycles and by the same formula but with $M = 1$ in case of simple life cycles.

(6) Based on these probabilities, randomly select the next mutant to be added to the community. Only one mutant can be added to the community at a time.

(7) Determine whether the selected mutant replaces the resident from which it originated or coexists with it. The latter case indicates an evolutionary branching point where the number of coexisting species increases by one. For this, we determine whether a mutant that carries a change in the same trait as the selected mutant but in opposite direction (e.g., $\boldsymbol{y} = (x_i^J, x_i^A + \epsilon)$ if the selected mutant is $\boldsymbol{y} = (x_i^J, x_i^A - \epsilon)$) has a positive establishment probability p_{est}.

(7.a) If yes, add the selected mutant to the community with initial density equal to half the density of the parental population and maintain the parental population at halve of its original density.

(7.b) If no, replace the parental population with the selected mutant with initial density equal to the density of the parental population.

(8) Return to (2) until T successful mutations have occurred. For complex life cycles we set $T = 4 \cdot 10^4$ whereas for simple life cycles we set $T = 2 \cdot 10^4$.

Community assembly through immigration

Community assembly through immigration is studied by successively adding new consumer species until the community is saturated. Each simulation is initialized with a single consumer species with randomly chosen trait vector, and its equilibrium density is determined by numerically solving the population dynamical equations (Eq. S2 for complex life cycles and Eq. S8 for simple life cycles). A new immigrant species with independently and randomly chosen juvenile and adult trait value is then added to the community given that it has a positive establishment probability as determined by Eq. (6), after which the equilibrium density of all species is computed again. Species with a density below an extinction threshold are removed from the community. This algorithm is iterated until no new immigrant species can successfully invade.

The simulation algorithm is programmed in C++ and implemented follows:

(1) Select a random trait vector (x^J, x^A) (x for simple life cycles) with trait values between -3 and 3 (this roughly delimits the set of possible trait vectors for which, given our choice of parameters, consumers can maintain a positive density).

(2) Check whether the selected trait vector is closer than a minimum Euclidean distance in trait space, set to 0.075, to any of the resident species.

(2.a) If yes, return to (1).

(2.b) If no, continue.

(3) Compute the establishment probability p_{est} for the selected trait vector.

(3.a) If $p_{\text{est}} < 0$, return to (1). If this occurs k times in a row the community is considered saturated and the simulation terminated. The values of k ranges, depending on the width of the feeding niche, between 60 and 100000 and is always chosen such that community saturation is certain.

(3.b) If $p_{\text{est}} > 0$, add a new species with the selected trait vector and initial density $(J, A) = (0.01, 0.01)$ to the community.

(4) Numerically solve Eq. (S2) for simple life cycles and Eq. (S8) for complex life cycles using Euler's forward method with a time increment of $t = 0.1$. We consider the system to have reached equilibrium once the difference between the density of every species present in the population before and after an iteration of the population dynamics is less than 10^{-7} or after a maximum of 10^5 iterations has been reached.

(5) Delete any lineage with a total density $(J + A)$ less than the extinction threshold, set to 0.004.

(6) Return to (1).

27

S6 Varying resource abundances

In this section, we investigate cases where we deviate from the assumption $k = k_J = k_A = 1$. First, to assure that the extraordinary species richness of communities with complex life cycles compared to communities simple life cycles in the immigration case is not due to case is not due to species with complex life cycles having twice the amount of total resources available, we here present results for the case $k = k_J + k_A = 2$. Figure S9 shows that doubling the amount of resources for species with simple life cycles increases the number of species in saturated communities for both gradual evolution and immigration. However, this increase is relatively small. Figure S5 confirms that it is the complex life cycle and not the increased total amount of resources that allows for high species richness with complex life cycles.

Next, we break the symmetry between k_J and k_A and investigate the cases $k_J = 0.67$, $k_A = 1.33$ and $k_J = 1.33$, $k_A = 0.67$. Figures S7 and S8 show the results for gradual evolution and immigration, respectively. These figures show that increasing k_J results in a wider interval of the adult trait space to be occupied while increasing k_A results in a wider interval of the juvenile trait space to be occupied. Decreasing these k-values has the opposite effect. The reason is that increasing k_J increases the maturation rate m while increasing k_A increases the birth rate. In the first case, the result is a higher density of juvenile individuals while in the second case the juvenile density increases. In both cases, increased population density increases the strength of competition, which is what drives increased character displacement. This pattern is most clearly visible for narrow niche width ($\sigma = 0.15$).
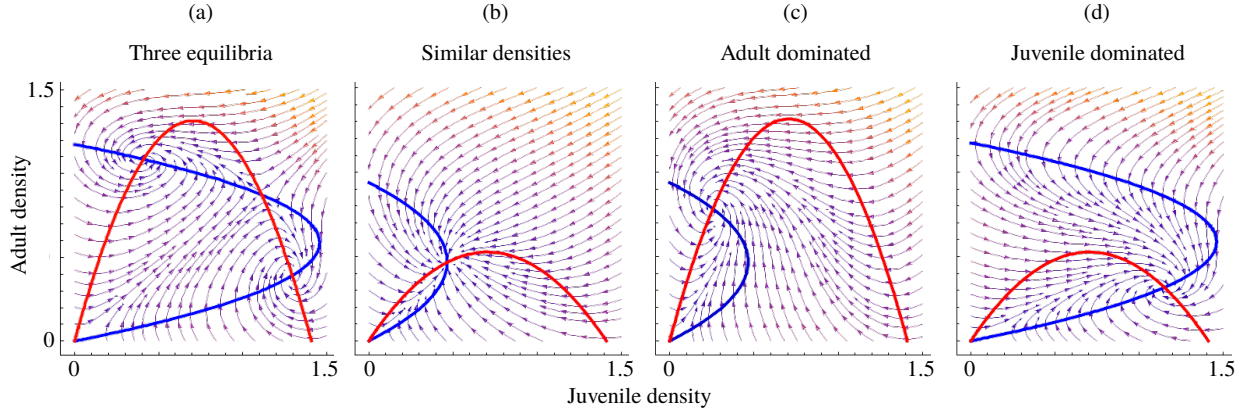
S7 Supplementary figures

Figure S1: Phase plane of the dynamical system given by Eq. (S2) for a single consumer species. The red curve shows the adult isocline and the blue curve the isocline for the total population density $(J + A)$. Besides the trivial equilibrium $(\hat{J}, \hat{A}) = (0, 0)$ the system can have, depending on parameter values, either three equilibria (panel a, here two stable equilibria separated by an unstable equilibrium) or one equilibrium (panel b-d, here stable). In case of a single equilibrium, the densities of juveniles and adults can be equal (b), adults can be more abundant than juveniles (c), or juveniles can be more abundant than adults (d). Here, we focus on the last scenario. For a more detailed analysis of a similar model see Schreiber & Rudolf (2008). Parameters: $x^J = 0$, $x^A = 0$, $\sigma_J = 0.15$, $\sigma_A = 0.15$. All other parameters as in Figure 2 except for (a) $c_J = 3.75$, $c_A = 6$, (b) $c_J = 1.5$, $c_A = 3$, (c) $c_J = 3.75$, $c_A = 3$, (d) $c_J = 1.5$, $c_A = 6$.
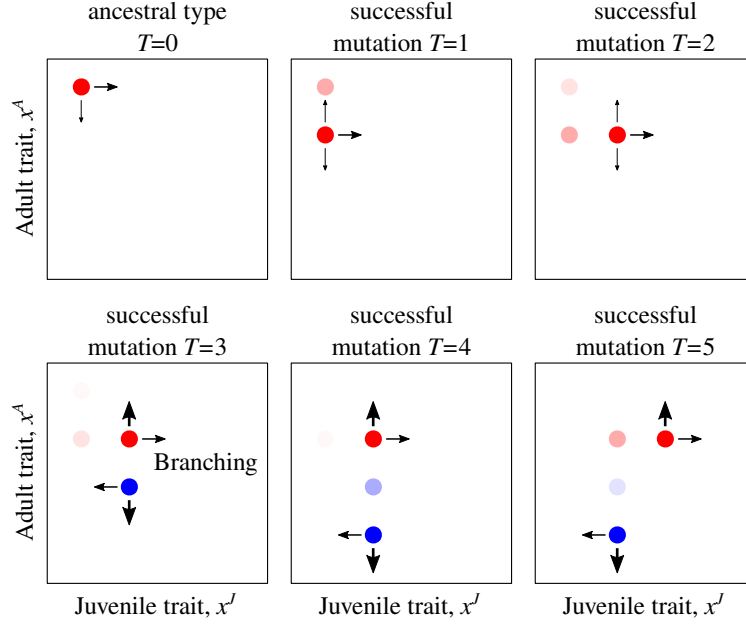
Figure S2: Schematic of an evolutionary trait substitution sequence with evolutionary branching. Dark red circles indicate the trait vector of a resident species while light circles indicate past trait vectors. Possible mutations with non-zero establishment probability are represented by arrows, the thickness of which represents the numerical value the rate of successful mutations $g(\boldsymbol{y}_i, \boldsymbol{X})$ (given by Eq. S26). The clock of the process T counts successful mutation events. At $T = 0$, only two mutants can establish from the ancestral type: a mutant that increases the juvenile trait value, and a mutant that decreases the adult trait value. The probability for each of them to establish before the other is proportional to the rate $g(\boldsymbol{y}_i, \boldsymbol{X})$. In our example, the mutation decreasing the adult trait value is selected as the $T = 1$ successful mutant, and this newly-arrived mutant replaces the resident. At this point, the species is at a branching point in the direction of the adult trait, as mutants with both higher and lower adult trait value have a positive establishment probability. The mutation that increases the juvenile trait value is selected as the $T = 2$ successful mutation. Next, the mutation that decreases the adult trait value is selected as the $T = 3$ successful mutation. Since the species is still at a branching point the newly-arrived mutant does not replace the resident but coexists with it, resulting in the addition of a second species to the community (blue circles). Further trait substitution results in a decreased adult trait value for the second species ($T = 4$) and in an increased juvenile trait value for the first species ($T = 5$).
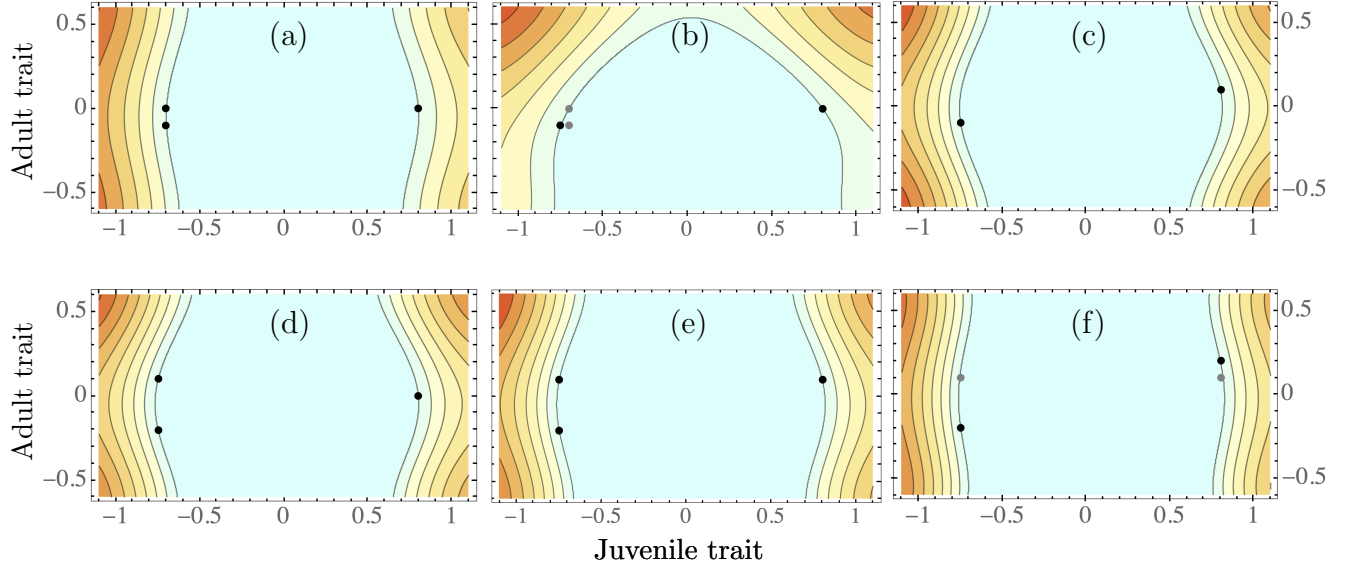
Figure S3: Two trait substitution sequences (a-c and d-f) illustrating alternative routes leading to a diagonal community. These sequences illustrate possible transitions from the community in Figure 5b to the community in Figure 5c in the main text. Figure 5b shows a community of two coexisting species with $\boldsymbol{x}_1 = (x_1^J, x_2^A) = (-0.7, 0)$ and $\boldsymbol{x}_2 = (0.8, 0)$, which experience directional selection on their juvenile trait in opposite directions, resulting in increased character displacement. The curvature of the contour lines indicates that both species also experience disruptive selection on their adult trait. Thus, any mutant differing in the adult trait can invade and coexist with its parental type. (a) A mutant with trait vector $\boldsymbol{x}_3 = (-0.7, -0.1)$ established itself. However, the resulting three-species community is generally transient. Based on the contour lines, mutants with more extreme juvenile trait values have a higher establishment probability than mutants affecting the adult trait value and adding either a mutant with trait vector $(-0.75, -0.1)$ or $(-0.75, 0)$ to the community results in the extinction of the species with trait vectors $\boldsymbol{x}_1$ and $\boldsymbol{x}_3$. This is shown in (b), where a mutant with trait vector $(-0.75, -0.1)$ had been added and where gray dots indicate extinct species. From now on the community is diagonal and this becomes more pronounced through subsequent trait substitutions as shown in (c). Alternatively, the two species on the left-hand side in (a) can continue to diverge in their adult trait values, leading to the community in (d) with $\boldsymbol{x}_1 = (-0.75, 0.1)$, $\boldsymbol{x}_2 = (0.8, 0)$ and $\boldsymbol{x}_3 = (-0.75, -0.2)$. Due to the asymmetry in the adult trait values of the species with $\boldsymbol{x}_1$ and $\boldsymbol{x}_3$, the species with trait vector $\boldsymbol{x}_2$ starts to experience directional selection in its adult trait, leading to $\boldsymbol{x}_2 = (0.8, 0.1)$ as shown in (e). As this species continues to specialize in its adult trait it will ultimately drive the species with trait vector $\boldsymbol{x}_1$ to extinction, again leading to a diagonal community (f).

31

	Number of species (structured case)						Number of species (unstructured case)	
0.75	8.1±0.3	6±0	4±0	4±0	2±0		3±0	0.75
0.60	8.6±0.5	6.2±0.4	4±0	4±0	2±0		4±0	0.60
0.45	10.1±0.3	7.3±0.5	6±0	4.9±0.3	4±0		5.8±0.4	0.45
0.30	12.8±0.9	8.4±0.8	6.7±0.8	5.9±0.3	3±0		8.6±0.8	0.30
σ_A ↑ 0.15	16.1±1.0	9.4±0.5	8.4±0.7	8±0	6.6±0.5		17.3±0.7	0.15 ↑ σ
	0.15	0.30	0.45	0.60	0.75			

σ_J →

Figure S4: Average species number and standard deviation from ten realizations of the gradual evolutionary dynamics. Numbers correspond to different combinations of σ_J and σ_A as indicated in the table margins and are identical to those in Figure 3. The tables for complex and simple life cycles are arranged such that the results for $\sigma_A = \sigma$ appear in the same row. Species are counted after $T = 4 \cdot 10^4$ successful mutations for complex life cycles and $T = 2 \cdot 10^4$ successful mutations for simple life cycles when communities were saturated. Parameters as in Figure 2.
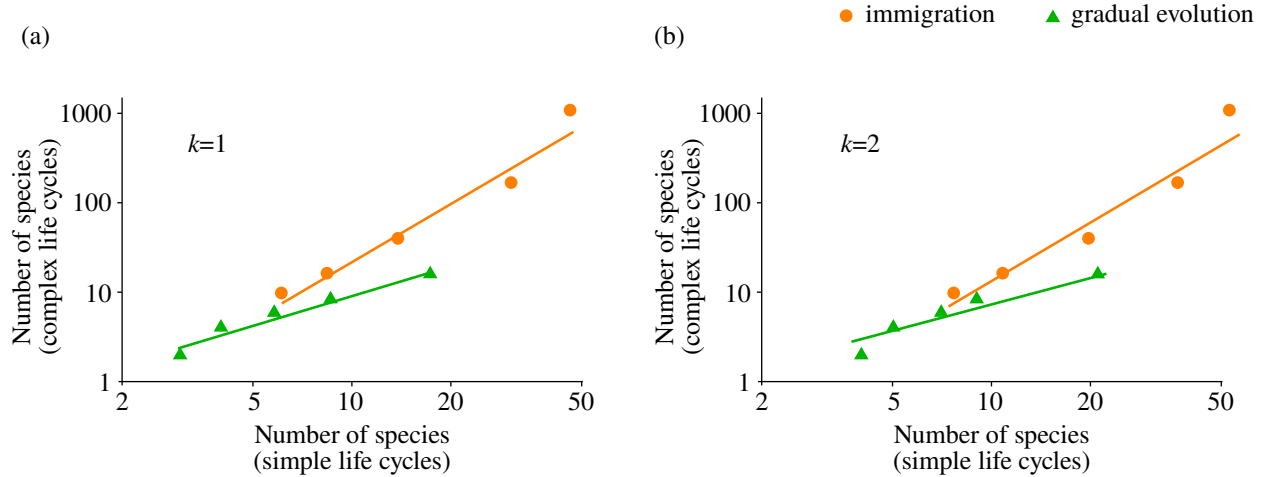

Figure S5: Log-log plot of the relationship in species richness between communities of species with simple (x-axis) and complex (y-axis) life cycles assembled through immigration (orange) and gradual evolution (green). (a) $k = k_J = k_A = 1$, (b) $k = 2$, $k_J = k_A = 1$. Symbols give averages over 10 simulation runs for, from left to right, decreasing values of $\sigma_J = \sigma = \sigma_A$ (same values as in Figure 4). Straight lines result from linear regression and indicate a power law with exponents (a) 2.2 and 1.1, and (b) 2.1 and 1.0, suggesting that the effect of doubling the amount of resources for communities of species with simple life cycle is marginal. Parameters as in Figure 2.
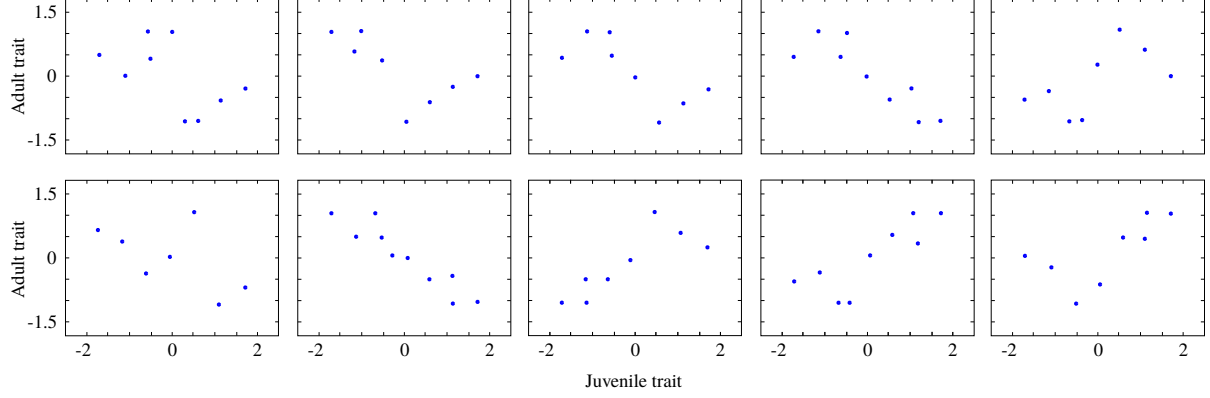
Figure S6: Composition of saturated communities resulting from gradual evolution. Panels show ten realizations for $\sigma_A = 0.3 = \sigma_J$. The variation between runs results from the stochasticity that acts during the establishment of new mutants. The second panel in the second row is identical to the corresponding panel in Figure 4b. Parameters as in Figure 2.
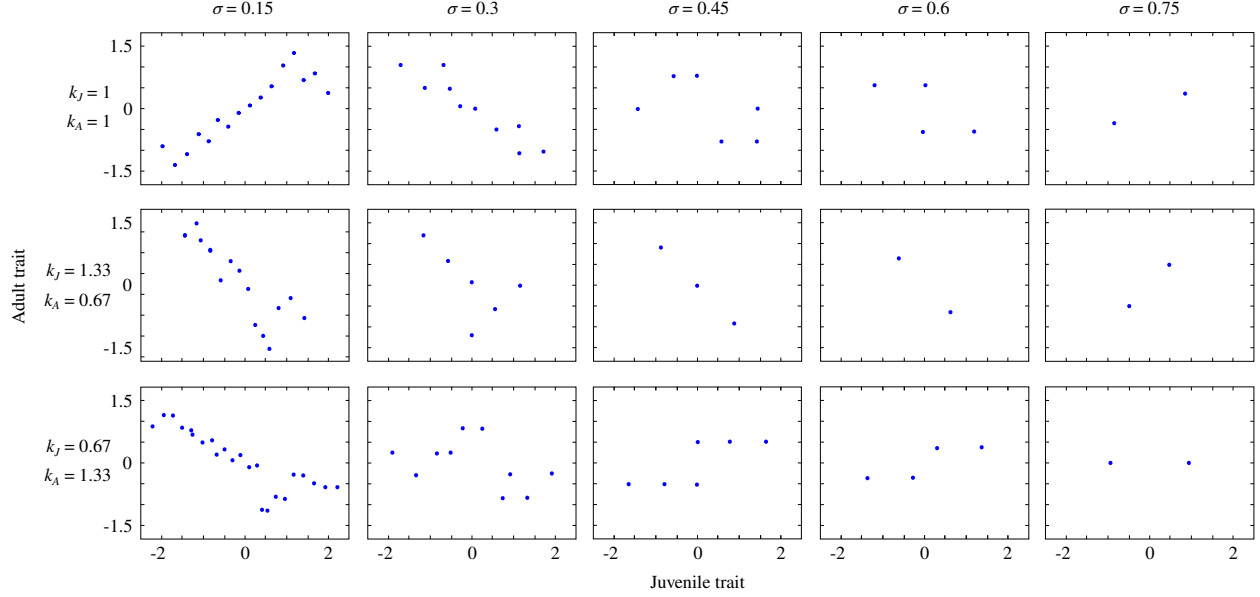

Figure S7: Composition of saturated communities resulting from gradual evolution for species with complex life cycles for five different values of the niche width σ. The first row is identical to Figure 4a and shows the case $k_J = 1 = k_A$. In the second and third row we break this symmetry and present the case $k_J = 1.33$, $k_A = 0.67$ and $k_J = 0.67$, $k_A = 1.33$, respectively. The other parameters are as in Figure 2.
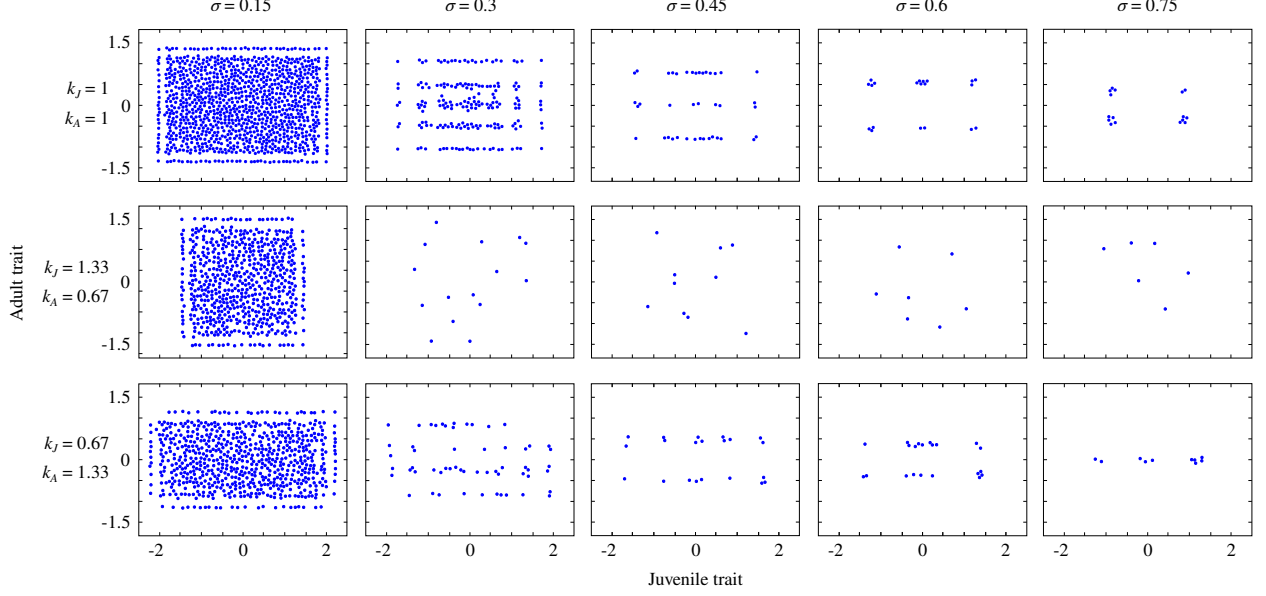
Figure S8: Composition of saturated communities resulting from immigration for species with complex life cycles for five different values of the niche width σ. The first row is identical to Figure 4c and shows the case $k_J = 1 = k_A$. In the second and third row we break this symmetry and present the case $k_J = 1.33$, $k_A = 0.67$ and $k_J = 0.67$, $k_A = 1.33$, respectively. The other parameters are as in Figure 2.
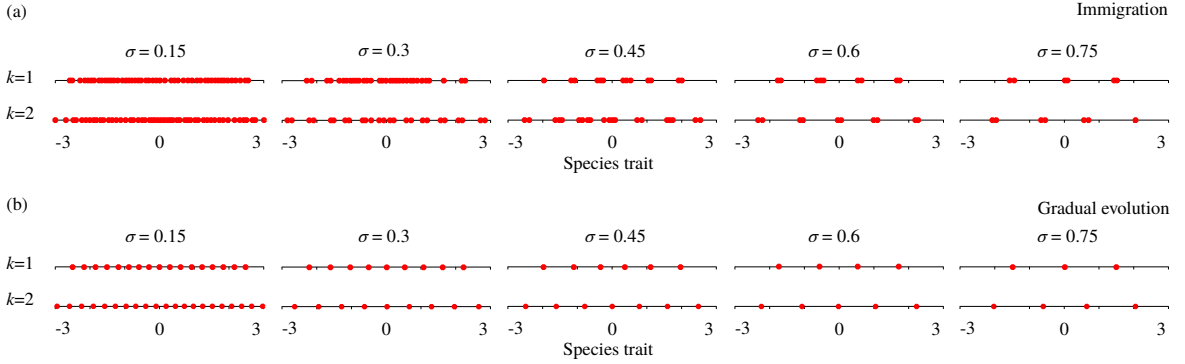

Figure S9: Composition of saturated communities resulting from (a) immigration and (b) gradual evolution for species with simple life cycles for five different values of the niche width σ. The first row in each panel is identical with Figure 4d and b, respectively, and shows the case $k = 1$. The second row shows the case $k = 2$. Doubling the amount of resources results in slightly more species-rich communities that occupy a slightly larger interval of the trait space. The other parameters are as in Figure 2.